Final Spatially-Constrained Inversions Report and Data Delivery for the Airborne Electromagnetic Survey of the Towner and Griggs Blocks, North Dakota for the North Dakota State Water Commission

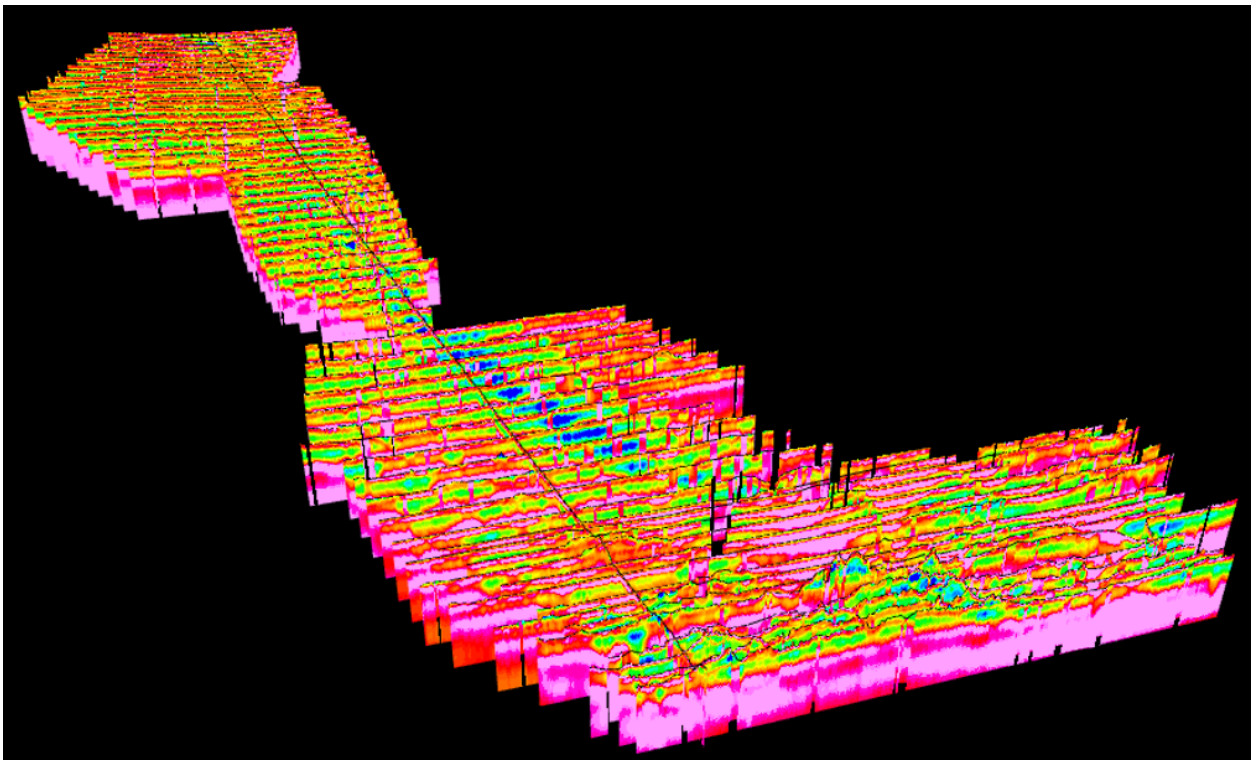

Jared Dale Abraham
Principle Geophysicist/Geologist
(303) 905-6240

Theodore H. Asch
Principle Geophysicist
(720) 415-7312

Aqua Geo Frameworks, LLC
130360 County Road D
Mitchell, NE 69357

March 9, 2020

Table of Contents

List of Figures

List of Tables

.

1. Introduction

The North Dakota State Water Commission (NDSWC) required a detailed hydrogeological framework of the Spiritwood Aquifer from north of Jamestown, North Dakota to the border of Manitoba Canada in order to implement ground water management plans. This is a continuation of a survey that was begun in 2016 in the Jamestown area (Legault et al., 2018) of the aquifer that continued in 2018 and early 2019 from the Jamestown area south to the South Dakota Border and also included a block area south of Devils Lake North Dakota in the Tolna area (Legault et al., 2019). The area in Manitoba was surveyed by the Canadian Geological Survey just north of the border and is summarized in Sapia et al. (2015). The desire of the NDSWC was to complete the mapping of the Spiritwood Aquifer from the border of Manitoba to the border of South Dakota. NDSWC contracted Geotech Ltd. (Geotech) to implement an Airborne Electromagnetic (AEM) survey of selected areas within North Dakota. Geotech contracted Aqua Geo Frameworks, LLC (AGF) to assist in the QA/QC and advanced processing and inversion of Geotech's Versatile Transient Electromagnetic (VTEM) systems data (Geotech, 2019). Specifically, AGF would conduct Laterally-Constrained Inversions (LCI) and Spatially-Constrained Inversions (SCI) of the VTEM data that would be compared to existing borehole data. The survey was implemented in two phases, one a regional reconnaissance acquisition and then infills planned based on preliminary results of the reconnaissance data.

The "as-flown" flight lines in the Towner and Griggs Block areas are presented in Figure 1-1 and Figure 1-2, respectively. Note that the Griggs and Towner Blocks are larger than the respective counties, but were used in the naming of these contiguous flight blocks.

2. Schedule/Time Line

Geotech mobilized to the Devil's Lake area on October 15, 2019. The system was assembled October 17-19, 2019 and ground tests and airborne tests were conducted on October 19 and 20th. Production began on October 24, 2019 and continued through November 18, 2019. Preliminary processing and LCI's were performed on the data from the October 25, 2019 until November 19, 2019 as data was made available from Geotech.

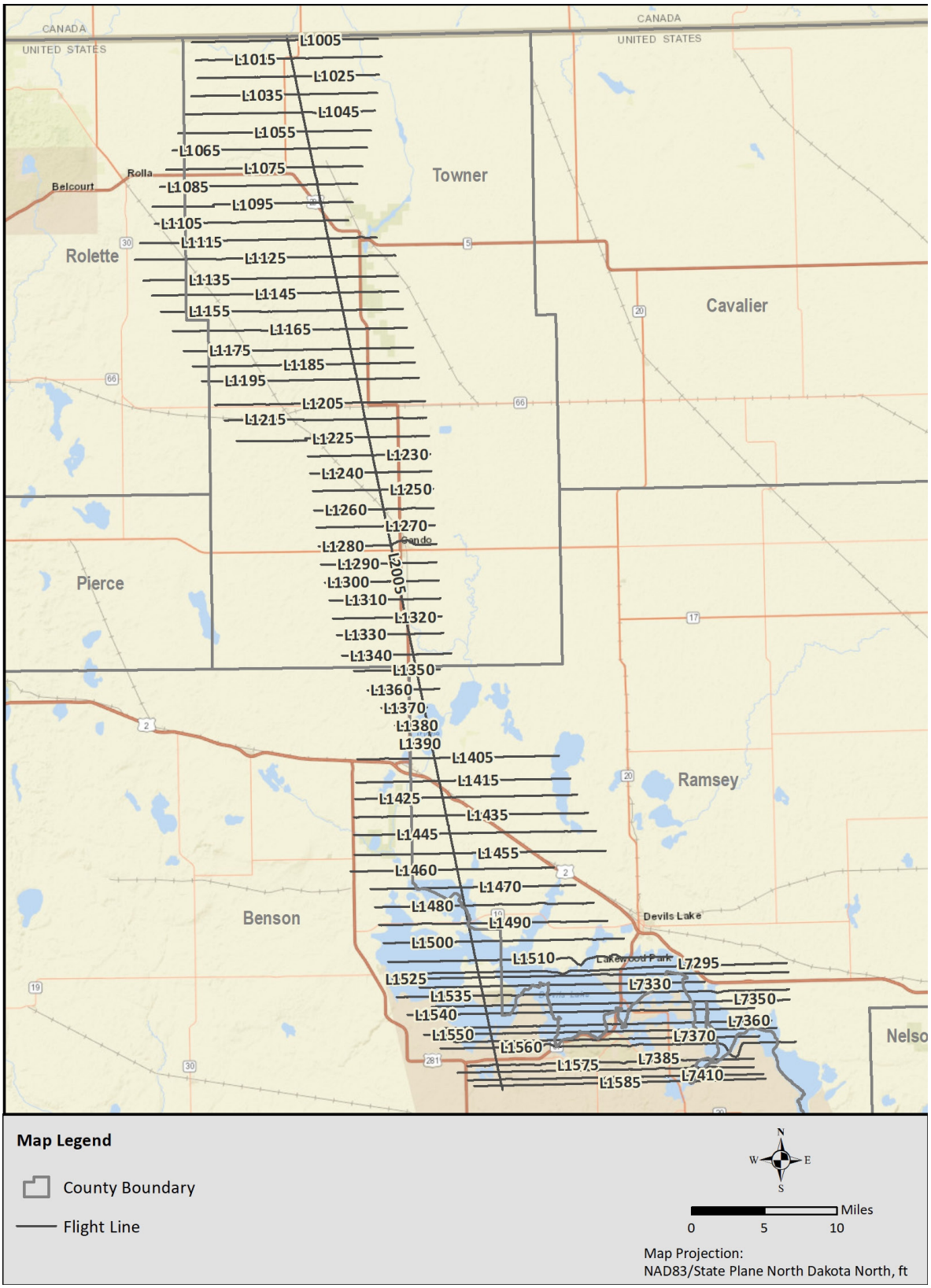

Figure 1-1. Final edited merged as-flown AEM VTEM-Plus data acquisition within the Towner Block area of North Dakota.

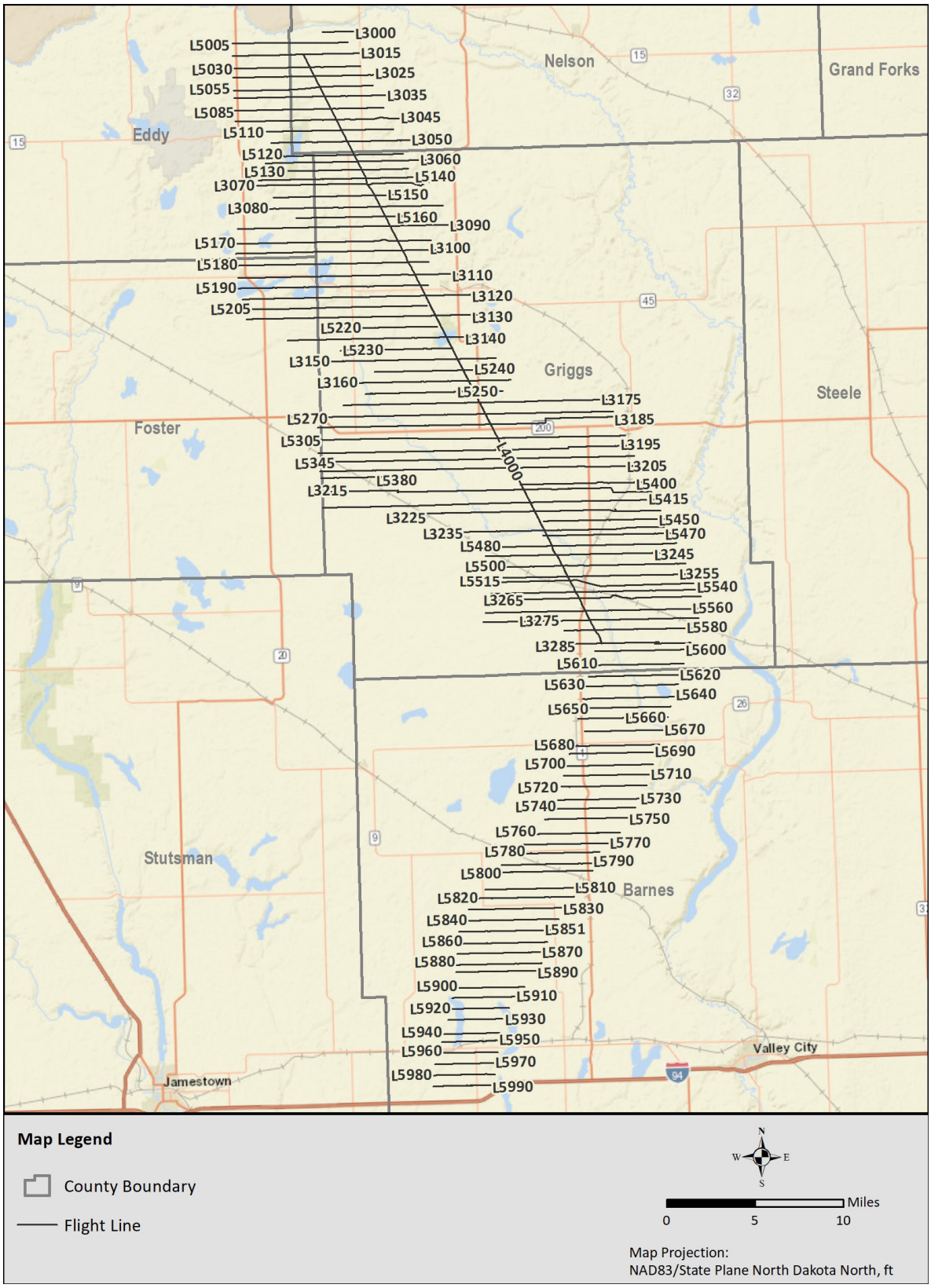

Figure 1-2. Final edited merged as-flown AEM VTEM-Plus data acquisition within the Griggs Block area of North Dakota.

3. System Calibration/Ground Tests

3.1 Test Line Calibration

The VTEM Plus system was flown over six known test holes locations (Griggs Block: 130934, 130935, 130368, 130941, and 130949) (Towner Block: 130950) with down-hole geophysical logs. The calibration process involves acquiring data with the system over the test hole locations. Acquired data are processed and a scale factor (time and amplitude) is applied so that the inversion process produces the model that approximates the known geology at the test hole locations. Final calibrations received from Geotech were applied to the data before the final SCI inversions.

3.2 System Ground Tests

Ground tests included checking for system operation including the following sub-systems: 1) transmitter (Tx) current amplitude and stability including waveform; 2) receiver (Rx) functionality 3) altimeter operation; 4) GPS operation; 5) altitude sensor operation and calibration; 6) navigation and communication; 7) airborne magnetometer operation; 8) base station magnetometer stability and field strength stability; and 9) DGPS base station operation.

3.3 System Airborne Tests

Airborne tests were conducted by Geotech to verify the operation of the system and are described in the Geotech report on the data acquisition.

3.4 Boreholes

Many borehole lithology logs were downloaded from the NDSWC Map Services (NDSWC, 2019), including both “Test Holes” and “Observation Wells”, for the general area of the survey. The boreholes were then down-sampled to only show the holes with the NDSWC ownership within the database. In addition to the downloaded lithology logs, NDSWC provided geophysical logs for test holes as noted above (Personal Communications, Rex Honeyman, Hydrologist NDSWC, October 16, 2019).

4. Data Acquisition

4.1 Acquisition Timing and as-flown lines

The NDSWC AEM data acquisition was flown out of the Devils Lake, Barnes County, and Rolla Municipal airports. The system was staged out of the Cando and Cooperstown Municipal Airports for some areas that required fuel stops. The production flights took place from October 24, 2019 to November 18, 2019. After the initial reconnaissance lines were flown in the Griggs Block, the Towner Block was flown. The Griggs infill and extension areas were flown based on the results of the preliminary LCI's of the VTEM Plus data as well as from an earlier 2016 VTEM survey of the Spiritwood area. Line-km totals from each flight are provided in Table 4-1. Note that the VTEM data in the databases are indexed by line and flight number. Figure 4-1 presents an "As Flown" map view of the reconnaissance and infill lines and the timing of the data collection. In some locations, the As-Flown lines deviate from the planned lines due to infrastructure and safety as determined by the pilot. The line totals were calculated from the preliminary databases using Geosoft Oasis montaj Total Distance GX (Geosoft, 2019)

Table 4-1. Flight line production by flight.

Date	Flights	Distance (km)	Distance (miles)
24-Oct-19	1, 2	208	129
25-Oct-19	3, 4	200	125
26-Oct-19	5	84	52
28-Oct-19	6, 7	184	114
31-Oct-19	8, 9	331	206
3-Nov-19	10, 11	332	206
5-Nov-19	12, 13	305	189
6-Nov-19	14, 15	220	137
7-Nov-19	16, 17	236	147
8-Nov-19	18, 19	256	159
11-Nov-19	20, 21	149	93
13-Nov-19	22	147	91
14-Nov-19	23	20	12
16-Nov-19	24	122	76
18-Nov-19	25, 26	234	146
	Total	3029	1882

4.2 System Flight Height Parameters

The system height was specified at ~30 meters; however, due to safety and other judgments by the pilot the flight heights will deviate. The goal was to maintain a height as low as possible in the window from 82 to 164 ft (25 to 50 m) above ground level (AGL). In the Griggs and Towner AEM data sets the average height was 122 ft (37.2 m) with a minimum of 69 ft (21.1 m) and a maximum of 491 ft (149.6) m. The maximum flight heights were encountered over large powerlines or other obstacles. Those data were removed from the dataset before inversion due to EM coupling so as to not impact the final product. A map of the flight heights throughout the survey area is presented in Figure 4-2.

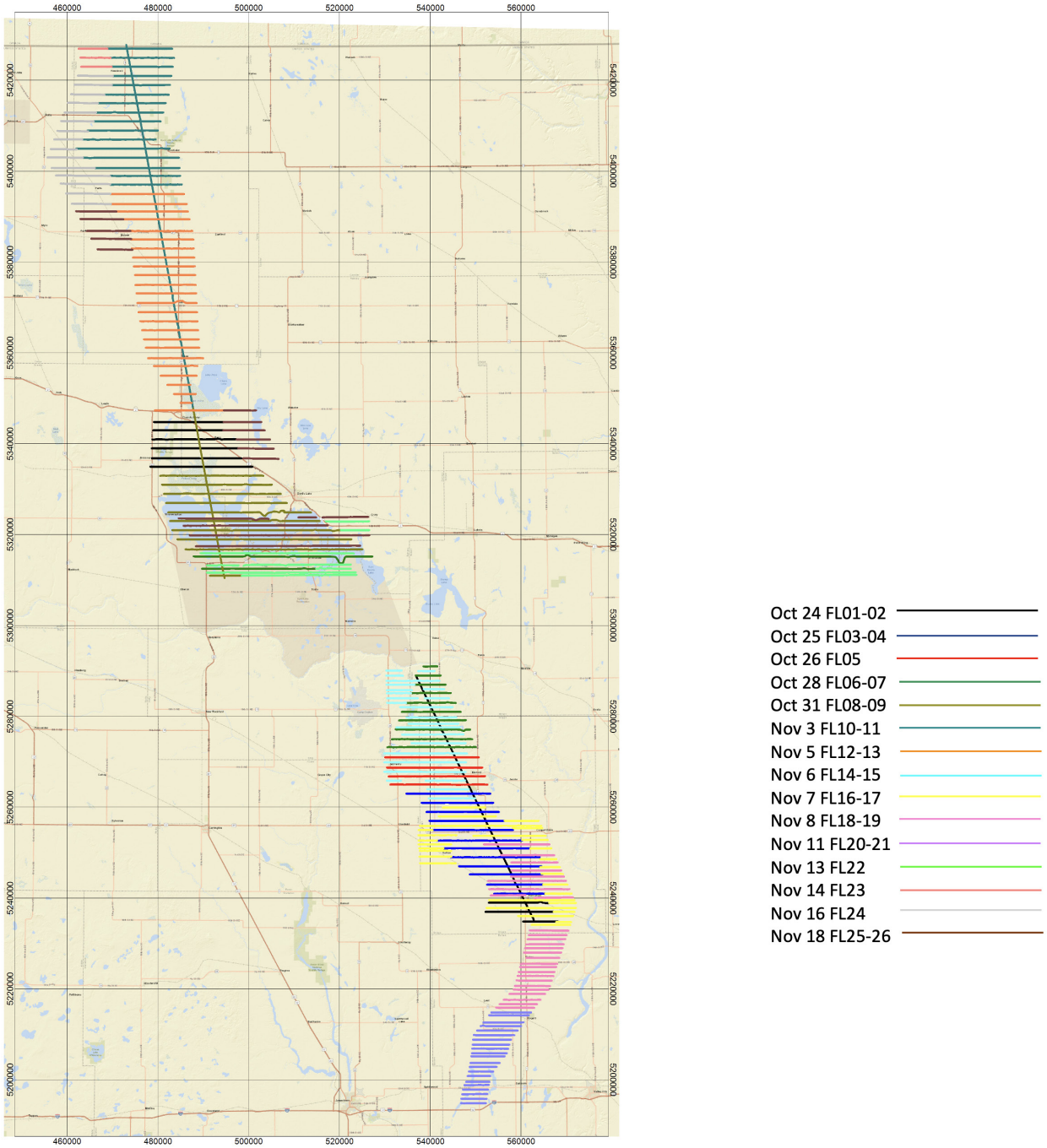

Figure 4-1. As-Flown map showing timing of the NDSWC Griggs and Towner Block AEM survey data acquisition.

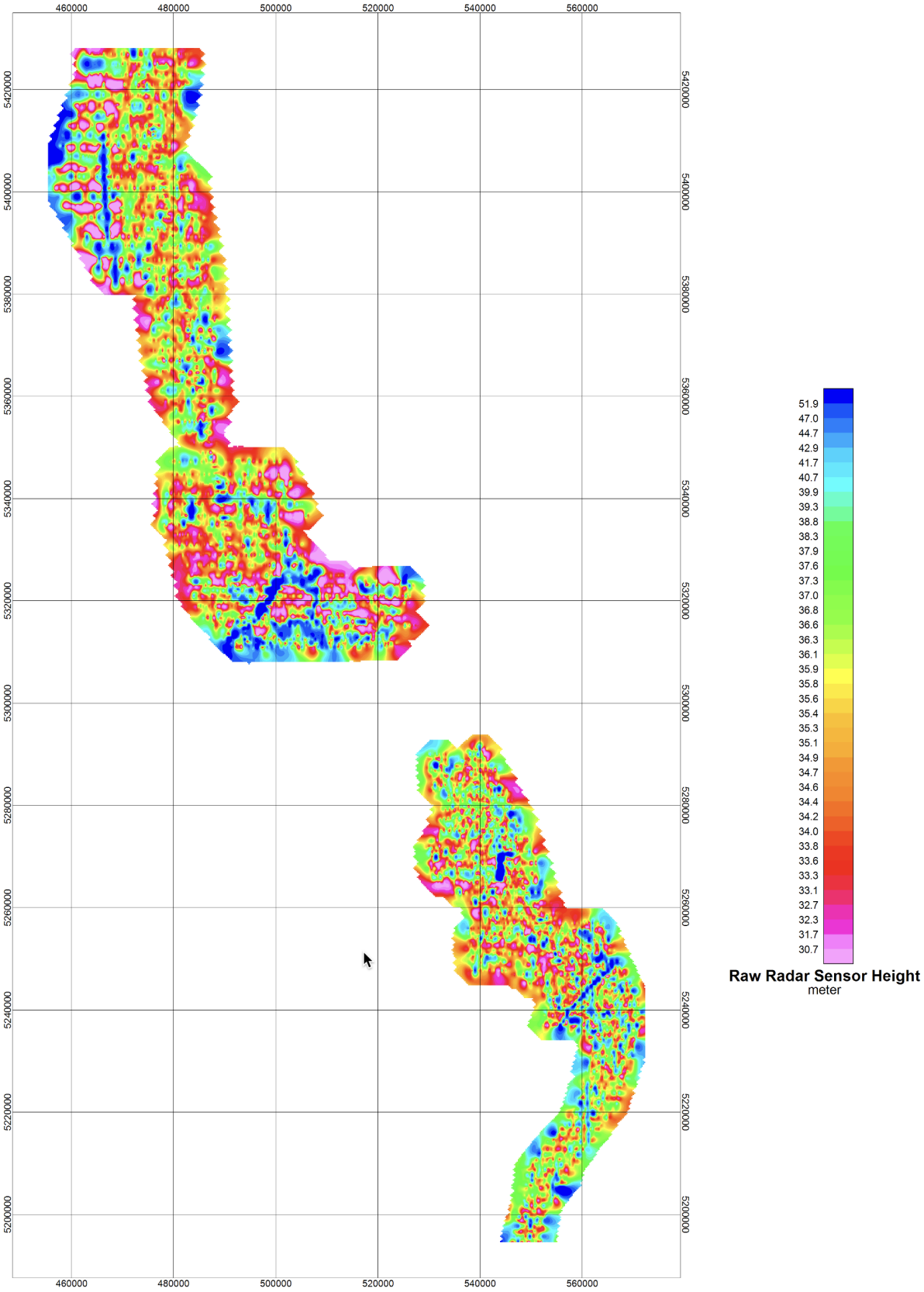

Figure 4-2. Map of the system height recorded during the NDSWC Towner and Griggs AEM survey.

4.3 Power Line Noise Intensity

The Geotech system is configured to record an estimate of the amplitude of the 60 Hz signals in the Power Line Monitor (PLM) channel. The PLM map is useful when investigating the impacts of powerlines on the data quality. The 60 Hz powerline signals have little impact on the Rx signal due to time-gating and proper filtering. However, the conductive wires that are used to transmit the power do cause EM coupling impacts on the data and those data need to be removed prior to inversion. The PLM for the 2019 Griggs-Towner AEM survey area is presented in Figure 4-3.

4.4 Magnetics

As part of the Geotech systems multiple Total Field magnetometers are included in the data acquisition package. The magnetic field signal is useful for determining deep seated geological contacts and is also extremely valuable for locating intrusive bodies. Neither of those was the target of the survey within the Griggs and Towner Blocks. However, the magnetic field is also sensitive to anthropogenic features that contain ferrous metal and is also used in the electromagnetic decoupling process. A plot of the magnetic Total Field intensity in the Griggs-Towner AEM survey area is presented in Figure 4-4. Both geological structure and cultural features can be identified within the survey area, but the signal is dominated by the complex basement features.

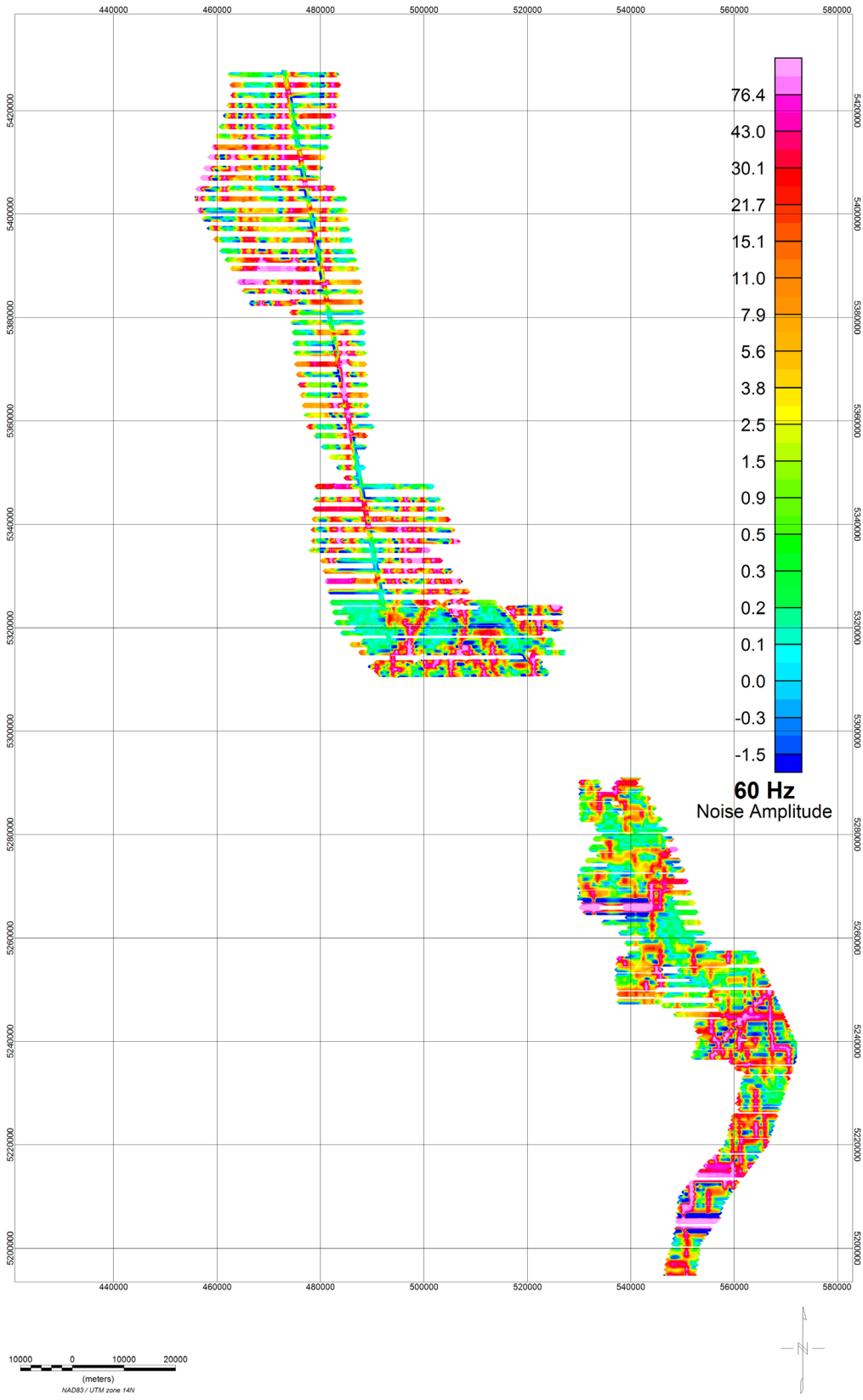

Figure 4-3. 60 Hz Power Line Monitor (PLM) intensity for the NDSWC Towner and Griggs AEM survey area.

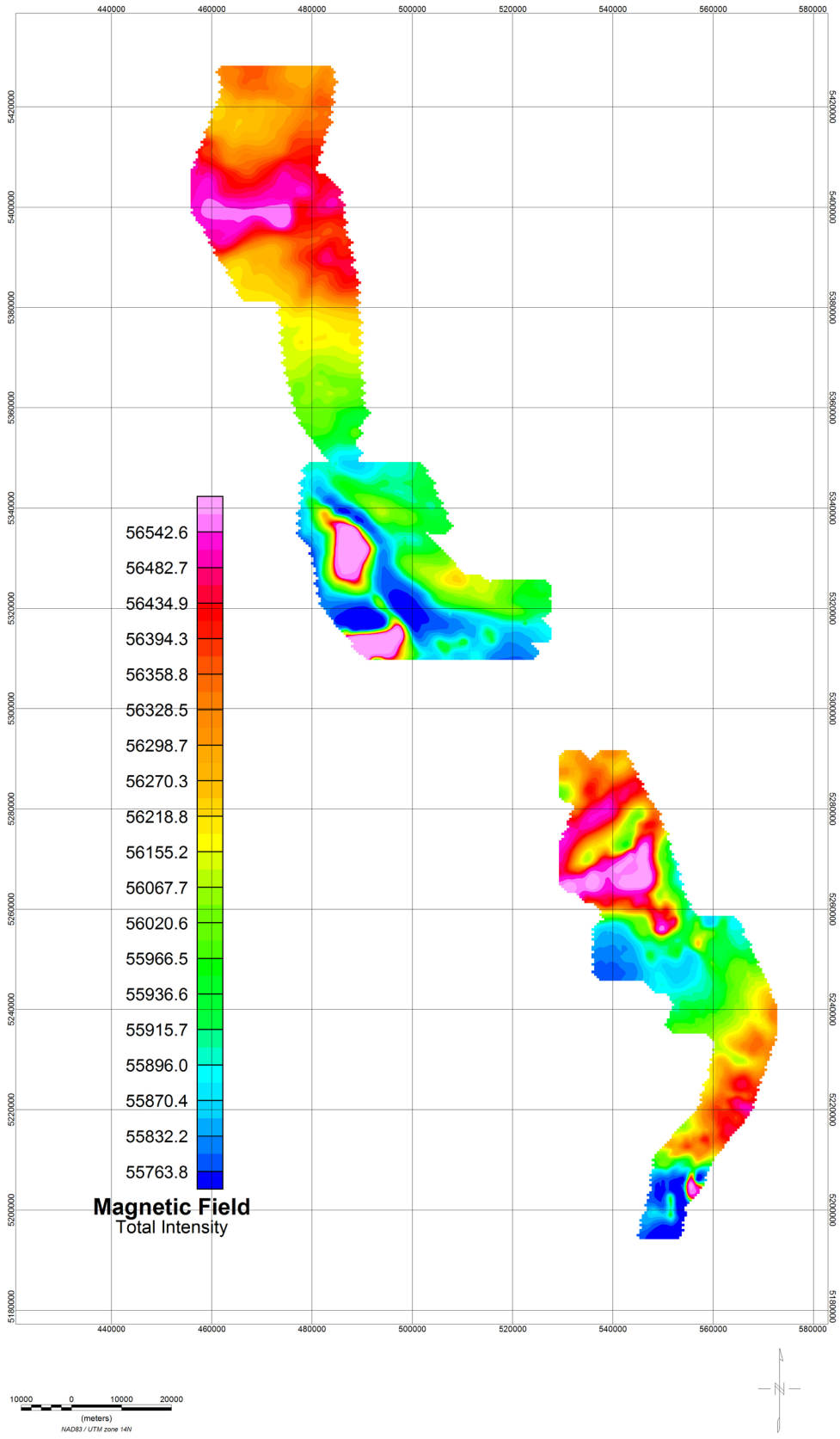

Figure 4-4. Magnetic Total Field Intensity for the NDSWC Griggs-Towner AEM survey area.

5. Processing and Laterally Constrained Inversions

5.1 Primary Field Processing

A standard Geotech data acquisition procedure involves review and processing of acquired raw data by Geotech in Canada. Details of that processing are provided in the Geotech acquisition report.

5.2 Automatic Processing

The AEM data were processed using Aarhus Workbench version 6.1.0 (Aarhus Geosoftware, 2020)

Automatic processing algorithms provided within the Workbench program are initially applied to the AEM data. DGPS locations were filtered using a stepwise, second-order polynomial filter of 7 seconds with a beat time of 0.5 seconds, based on flight acquisition parameters. The altitude data were corrected using a series of two polynomial filters. The lengths of the eighth-order polynomial filters were set to 15 seconds and 12 seconds with shift lengths of six (6) seconds. The lower and upper thresholds were 1 and 100 meters, respectively.

Trapezoidal spatial averaging filters were next applied to the AEM data. The times used to define the trapezoidal filters for the VTEM data were $1.0x10^{-5}$ sec, $1.0x10^{-4}$ sec, and $1.0x10^{-3}$ sec with widths of 1, 3, and 5 seconds. The trapezoid sounding distance was set to 1.0 seconds and the left/right setting, which requires the trapezoid to be complete on both sides, was turned on. The spike factor and minimum number of gates (as a percent (%)) were both set to 20 percent.

5.3 Manual Processing and Laterally-Constrained Inversions

After the implementation of the automatic filtering, the AEM data were manually examined using a sliding two-minute time window. The data were examined for possible electromagnetic coupling with surface and buried utilities and metal, as well as for late time-gate noise. Data affected by these were removed. Areas were also cut out where the system height was flown greater than approximately 65 m (213 ft) above the ground surface which caused a decrease in the signal level.

The AEM data were then inverted using a Laterally-Constrained Inversion (LCI) algorithm (Aarhus Geosoftware, 2019). The LCI uses nearby soundings along the flight lines as constraints. The profile and depth slices were examined, and any remaining electromagnetic couplings were masked out of the data set. Vertical constraints on the resistivity were set at 2.7 and at 1.5 for the horizontal resistivity constraints with a reference distance of 100 m (328 ft) and a fall off power of 0.75. The data were processed, edited, and inverted as they became available with the goal of having the analysis of each day's acquired data completed before the next data became available. The smooth model 40-layer structure used in the LCI inversions is presented in Table 5-1.

Table 5-1. Thickness and depth to bottom for each layer in the AEM earth models for the Laterally-(LCI) and Spatially-Constrained (SCI) inversions. The thickness of the model layers increase with depth as the resolution of the AEM technique decreases.

Layer	Depth to Bottom (ft)	Thickness (ft)	Depth to Bottom (m)	Thickness (m)	Layer	Depth to Bottom (ft)	Thickness (ft)	Depth to Bottom (m)	Thickness (m)
1	9.8	9.8	3.0	3.0	21	343.1	25.1	104.6	7.7
2	20.1	10.3	6.1	3.1	22	369.3	26.2	112.6	8.0
3	31	10.9	9.4	3.3	23	396.8	27.5	120.9	8.4
4	42.3	11.3	12.9	3.4	24	425.6	28.8	129.7	8.8
5	54.2	11.9	16.5	3.6	25	455.8	30.2	138.9	9.2
6	66.6	12.4	20.3	3.8	26	487.4	31.6	148.6	9.6
7	79.6	13	24.3	4.0	27	520.6	33.2	158.7	10.1
8	93.3	13.7	28.4	4.2	28	555.3	34.7	169.2	10.6
9	107.6	14.3	32.8	4.4	29	591.7	36.4	180.3	11.1
10	122.5	14.9	37.3	4.5	30	629.8	38.1	192.0	11.6
11	138.2	15.7	42.1	4.8	31	669.7	39.9	204.1	12.2
12	154.7	16.5	47.2	5.0	32	711.6	41.9	216.9	12.8
13	171.9	17.2	52.4	5.2	33	755.5	43.9	230.3	13.4
14	190	18.1	57.9	5.5	34	801.4	45.9	244.3	14.0
15	208.9	18.9	63.7	5.8	35	849.6	48.2	258.9	14.7
16	228.7	19.8	69.7	6.0	36	900.1	50.5	274.3	15.4
17	249.5	20.8	76.0	6.3	37	952.9	52.8	290.4	16.1
18	271.3	21.8	82.7	6.6	38	1008.3	55.4	307.3	16.9
19	294.1	22.8	89.6	6.9	39	1066.4	58.1	325.0	17.7
20	318	23.9	96.9	7.3					

6. Spatially-Constrained Inversions

Following the initial EM decoupling and LCI analysis and then the releveling analysis performed by Geotech, the Towner and Griggs AEM data were again processed and edited to remove power line effects. This resulted in about 1,576.2 line-km (973.0 line-miles) of data retained for inversion for the Towner AEM area and 1,262.1 line-km (779.1 line-miles) of data retained for inversion for the Griggs AEM area. This amounts to a retention rate of about 94.6% for the Towner AEM area and a 90.6% retention rate for the Griggs AEM survey area. A visual image of a comparison of the as flown data for the Towner area to the data retained for the SCI inversions is presented in Figure 6-1. A similar image of the data retained for inversion is presented in Figure 6-2 for the Griggs AEM survey area.

After processing and editing of the data, Spatially-Constrained Inversions (SCI) were performed. Note that SCI's use AEM data along, and across, flight lines within a user-specified distance criteria (Viezzoli et al., 2008) versus the LCI where only data along a given flight line are used as constraints. The NDSWC AEM data were inverted using smooth models with 40 layers, each with a starting resistivity of 5 ohm-m (equivalent to a 5 ohm-m halfspace). The thicknesses of the first layers of the models were about 10 ft with the thicknesses of the consecutive layers increasing by a factor of about 1.08 (Table 5-1). The depths to the bottoms of the 39th layers were set to 1,066 ft (325 m), with thicknesses up to about 58 ft (~18 m). The thicknesses of the layers are set to increase with depth as the resolution of the technique decreases. The spatial reference distance for 100% constraint was set to 328 ft (100 m) with a power law fall-off of 0.75. The vertical and lateral constraints, ***ResVerSTD*** and ***ResLatStD***, were set to 2.4 and 1.4, respectively, for all layers. These parameters provided both a reasonable and constrained, yet smooth, result.

In addition to the recovered resistivity models the SCIs also produce data residual error values (single sounding error residuals) and Depth of Investigation (DOI) estimates. The data residuals compare the measured data with the response of the individual inverted models (Christensen et al., 2009). The DOI provides a general estimate of the depth to which the AEM data are sensitive to changes in the resistivity distribution at depth (Christiansen and Auken, 2012). Two DOI's are calculated: a "Conservative" DOI at a cumulative sensitivity of 1.2 and a "Standard" DOI set at a cumulative sensitivity of 0.6. A more detailed discussion on the DOI can be found in Asch et al. (2015).

Figure 6-3 presents a histogram of the Towner AEM SCI inversion data/model residuals and Figure 6-4 presents a histogram of the Griggs AEM SCI inversion data/model residuals. A Google Earth map of the SCI data residuals for the Towner AEM study area is presented in Figure 6-5 and a similar image of the data/model residuals for the Griggs AEM study area is presented in Figure 6-6.The residual error equals, per sounding, the square root of the sum of the square of the true data minus the model value divided by the true data (Auken et al., 2015; Christiansen et al., 2016). What is important to note on these residual plots is that while there is a distribution of residual error between 0.18 and 0.37 for the Towner Block area and 0.18 and 0.45 for the Griggs Block area, the maximum amplitudes of the SCI residual error for both these areas is quite low. Typical residual errors are usually in the range of 0.50 -0.80. The errors for Towner and Griggs are about half of those more common error ranges. Typically, higher errors occur over power lines which are usually located along roads and river channels. That is likely what can be observed over the Towner Block in Figure 6-5.

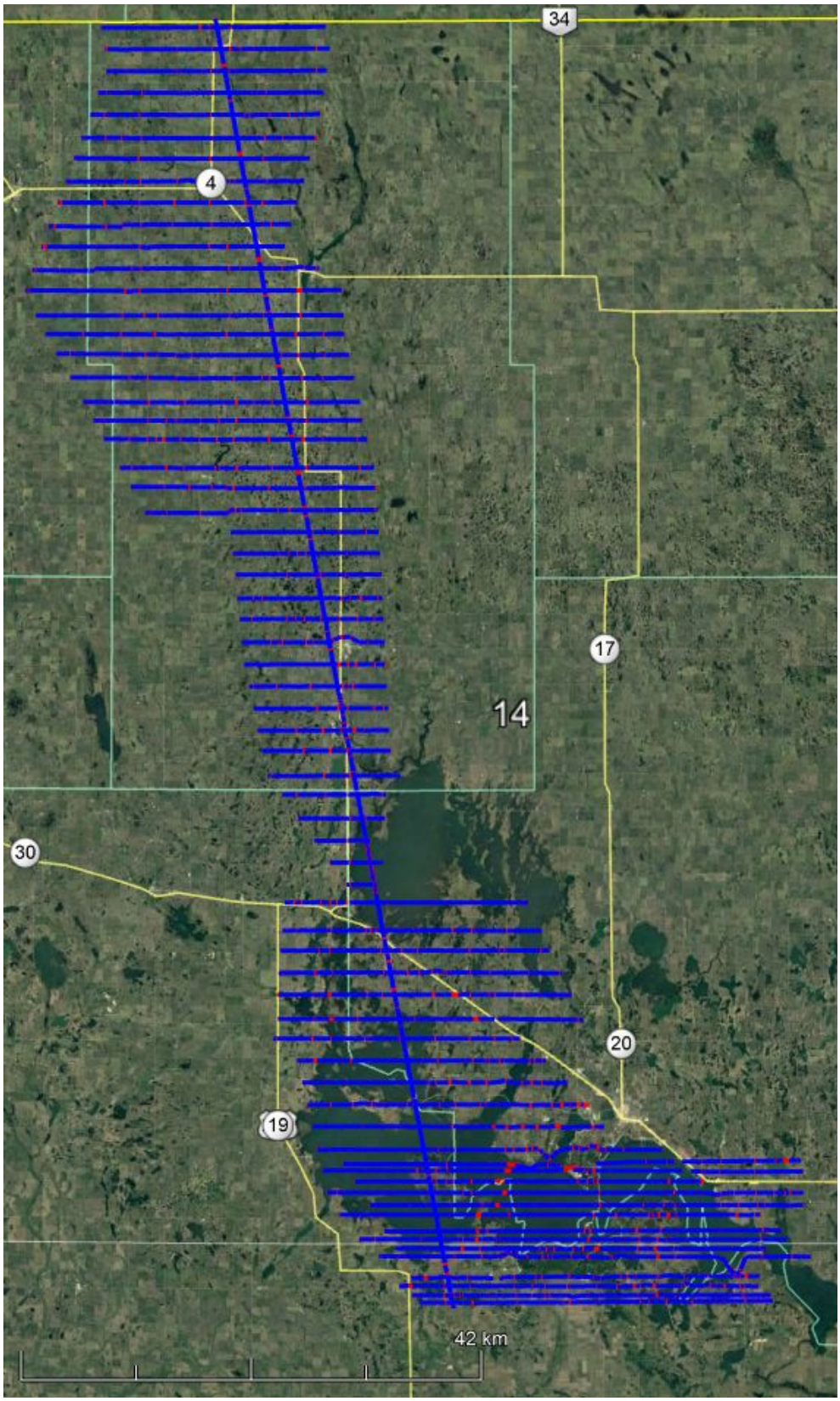

Figure 6-1. Comparison of the acquired data (red) versus the final retained data (blue) for the NDSWC Towner AEM survey area Final SCI inversion. This kmz is included in Appendix 3 Deliverables\KMZ.

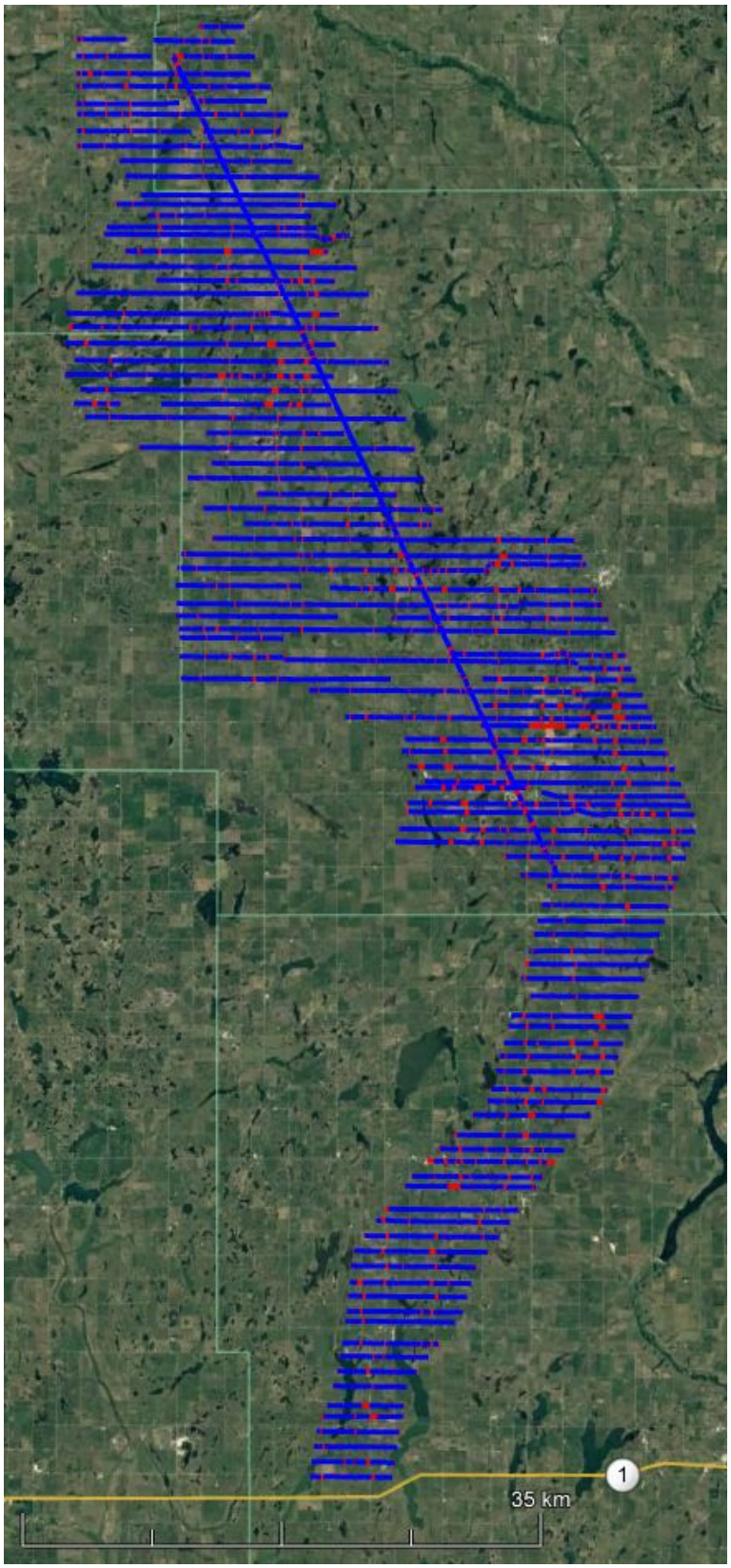

Figure 6-2. Comparison of the acquired data (red) versus the final retained data (blue) for the NDSWC Griggs AEM survey area Final SCI inversion. This kmz is included in Appendix 3 Deliverables\KMZ.

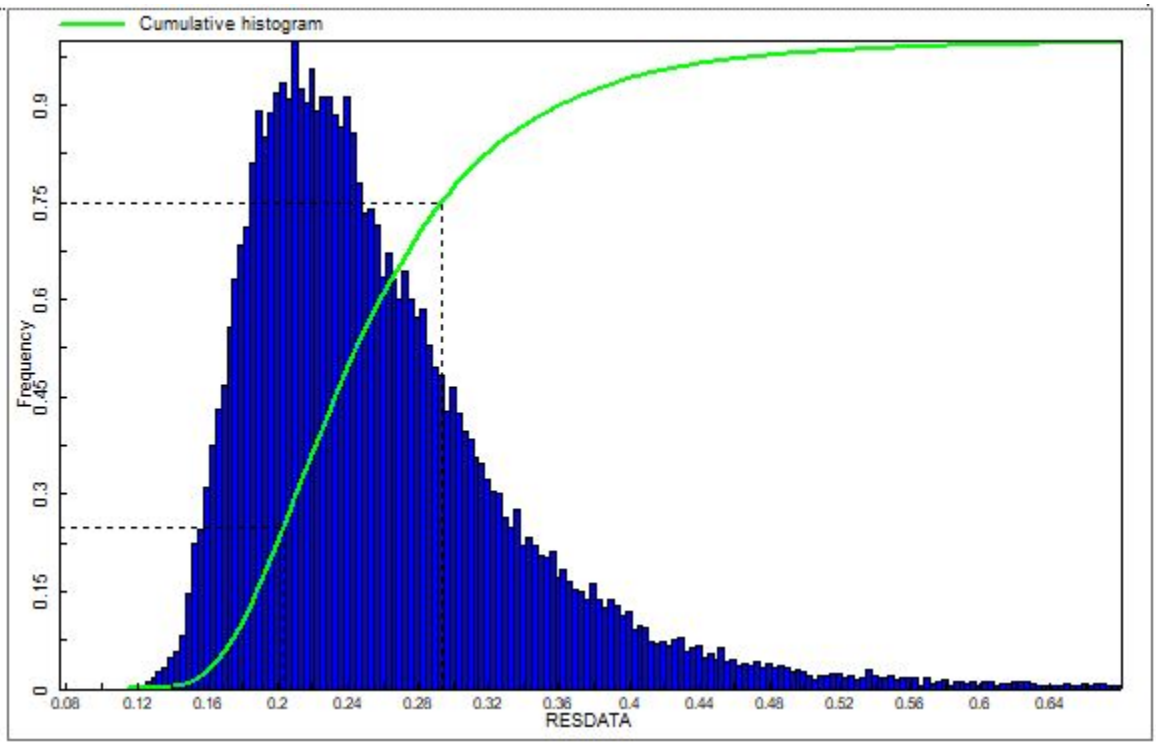

Figure 6-3. Data/model residual histogram for the NDSWC Towner SCI inversion results.

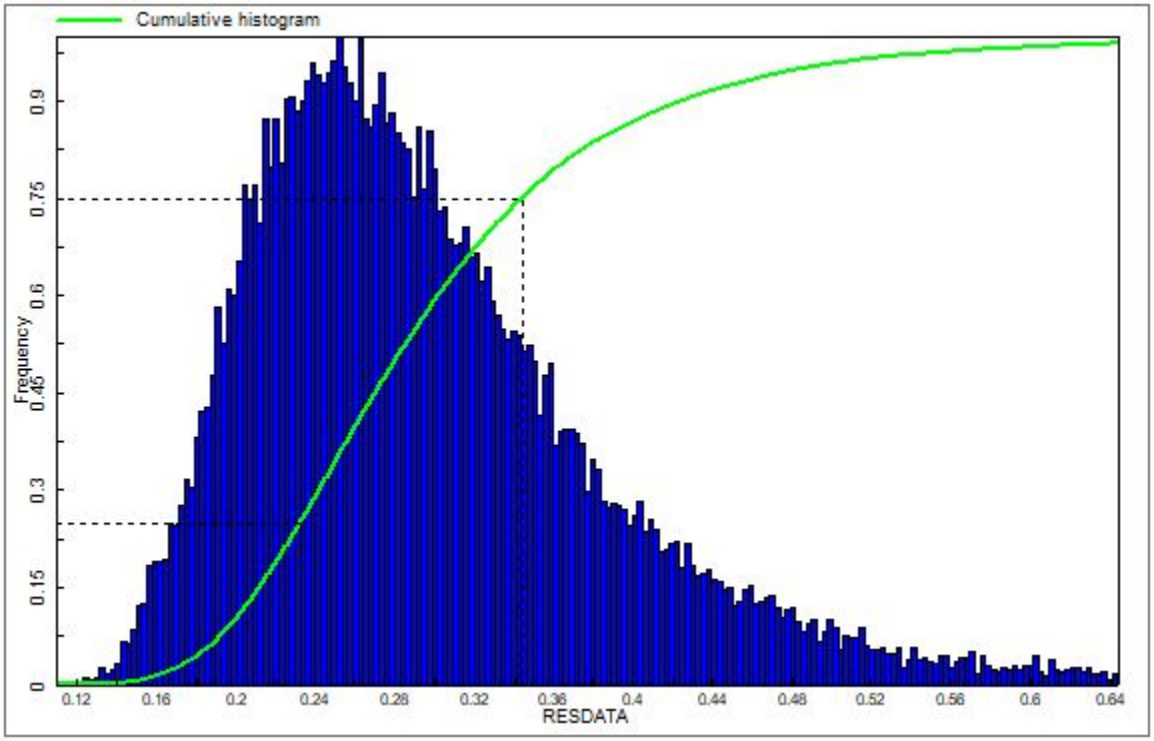

Figure 6-4. Data/model residual histogram for the NDSWC Griggs SCI inversion results.

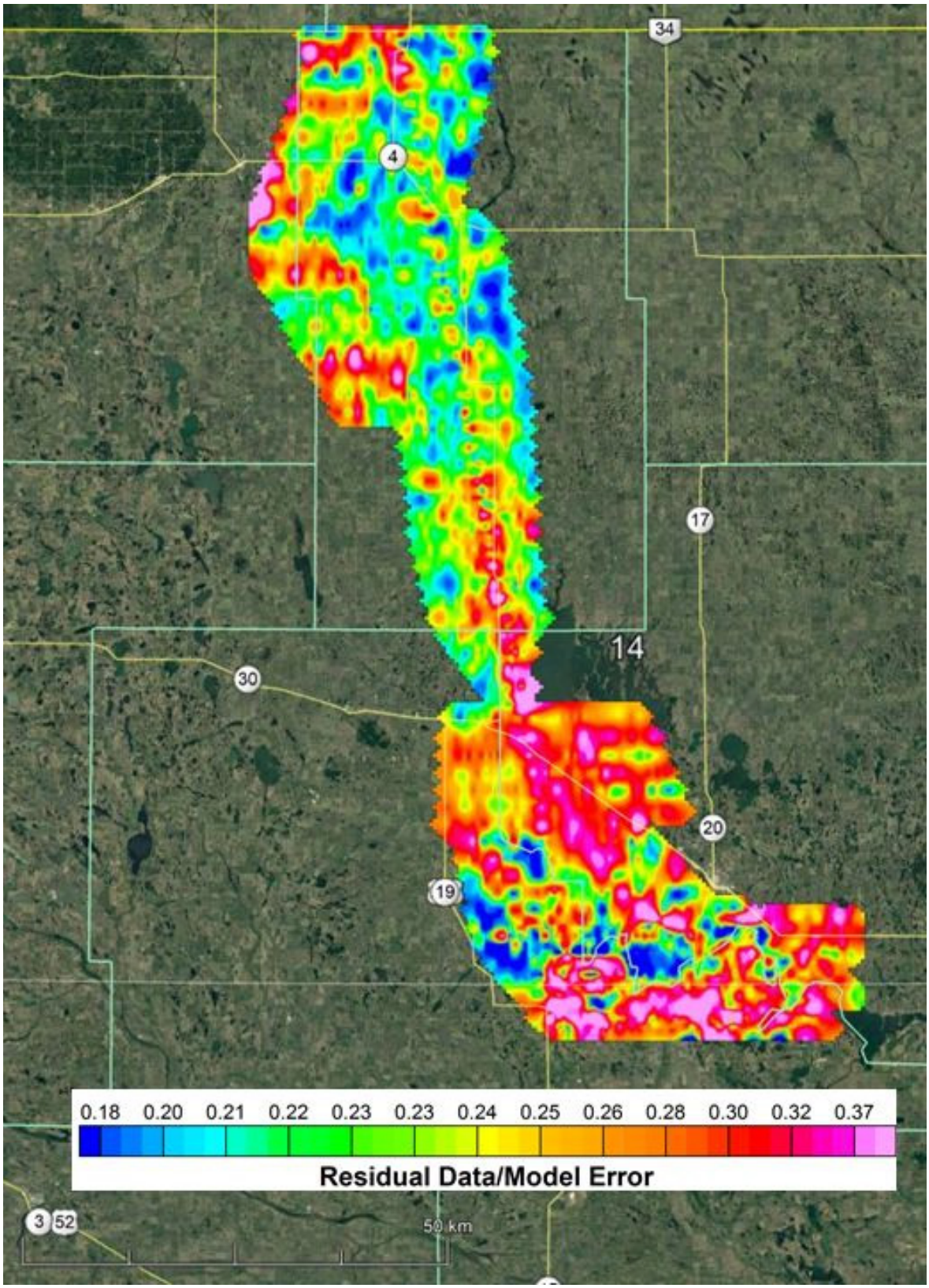

Figure 6-5. Map of data residuals for the Towner AEM SCI inversion results plotted in Google Earth. These data are included as a Google Earth KMZ file in Appendix 3.

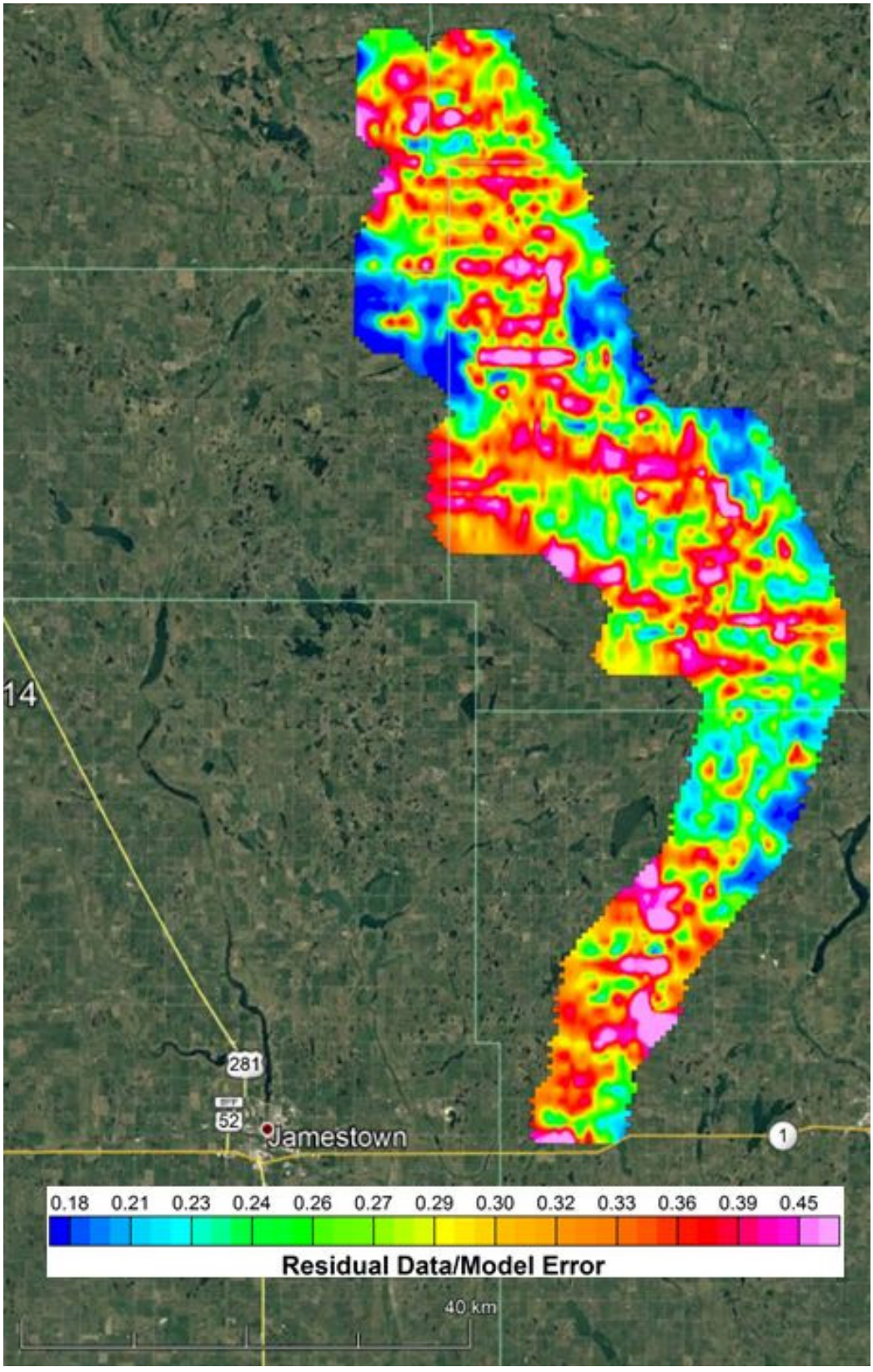

Figure 6-6. Map of data residuals for the Griggs AEM SCI inversion results plotted in Google Earth. These data are included as a Google Earth KMZ file in Appendix 3.

7. Comparison of AEM Inversion Results to Boreholes

7.1 Merging Lines

After the inversion process several short lines and line segments were combined to form continuous lines within the Towner and Griggs Blocks AEM survey areas. These merged lines allow for improved viewing and interpretation of the AEM inversions results. Table 7-1 lists the original lines and the new combined lines for the Towner Block survey area. Table 7-2 lists the original lines and the new combined lines for the Griggs Block survey area. For lines that have overlapping data (examples are the line extensions or the test lines), the overlapping regions of the flight lines were sorted in the dominant (east-west or north-south) line direction and combined. This has no impact on the SCI as the actual X, Y, and Z locations of the survey data are used in the inversions.

7.2 Construct the Project Digital Elevation Model

To ensure that the elevation used in the project is constant for all the data sources (i.e. boreholes and AEM) a Digital Elevation Model (DEM) was constructed for the NDSWC Towner Block AEM survey area and for the Griggs Block AEM survey area. The data were downloaded from the National Elevation Dataset (NED) located at the National Map Website (U.S. Geological Survey, 2019) at a resolution of 1 arc-second or approximately 100 ft. The geographic coordinates for the Towner Block survey area are in North American Datum of 1983 (NAD83), State Plane North Dakota North (International foot), and the elevation values are referenced to the North American Vertical Datum of 1988 (NAVD 88) (in feet). The geographic coordinates for the Griggs survey area are in North American Datum of 1983 (NAD83), State Plane North Dakota North (International foot), and the elevation values are referenced to the North American Vertical Datum of 1988 (NAVD 88) (feet). The southern portion of the Griggs Block extends into the NAD83, State Plane North Dakota South (International foot) zone but was projected in NAD83 State Plane North Dakota North (International foot), and the elevation values are referenced to the NAVD 88 (feet) in order to facilitate plotting and gridding of results. The 100 ft grid cell size was used throughout the project and resulting products. Figure 7-1 is a map of the DEM of the NDSWC Towner Block and Griggs Block AEM survey areas. The vertical relief of the topography under the flight lines for Towner was 366 ft with a minimum elevation of 1430 ft and a maximum elevation of 1796 ft. The vertical relief of the topography under the Griggs flight lines was 408 ft with a minimum elevation of 1312 ft and a maximum elevation of 1720 ft. These respective DEM's were used to reference all elevations within the survey areas. The ArcView Binary Floating-Point Raster file (*.flt) and can be found in *Appendix 3 Deliverables\Grids\ DEM*.

Table 7-1. Combination of flight lines within the Towner Block AEM Survey Area.

Original Source Lines	Direction	New Line
L1000, and L7000	East-West	L1005
L1010, and L7010	East-West	L1015
L1020, and L7020	East-West	L1025
L1030, and L7030	East-West	L1035
L1040, and L7040	East-West	L1045
L1050, and L7050	East-West	L1055
L1060, and L7060	East-West	L1065
L1070, and L7070	East-West	L1075
L1080, and L7080	East-West	L1085
L1090, and L7090	East-West	L1095
L1100, and L7100	East-West	L1105
L1110, and L7110	East-West	L1115
L1120, and L7120	East-West	L1125
L1130, and L7130	East-West	L1135
L1140, and L7140	East-West	L1145
L1150, and L7150	East-West	L1155
L1160, and L7160	East-West	L1165
L1170, and L7170	East-West	L1175
L1180, and L7180	East-West	L1185
L1190, and L7190	East-West	L1195
L1200, and L7200	East-West	L1205
L1210, and L7210	East-West	L1215
L1220, and L7220	East-West	L1225
L1400, and L7230	East-West	L1405
L1410, and L7240	East-West	L1415
L1420, and L7250	East-West	L1425
L1430, and L7260	East-West	L1435
L1440, and L7270	East-West	L1445
L1450, and L7280	East-West	L1455
L1520, and L7320	East-West	L1525
L1530, and L7340	East-West	L1535
L1570, and L7400	East-West	L1575
L1580, and L7420	East-West	L1585
L2000, and L2001	North-South	L2005
L7290, L7300, and L7310	East-West	L7295

L7380, and L7390	**East-West**	**L7385**

Table 7-2. Combination of flight lines within the Griggs Block AEM Survey Area.

Original Source Lines	Direction	New Line
L3010, and L5020	**East-West**	**L3015**
L3020, and L5040	**East-West**	**L3025**
L3030, and L5070	**East-West**	**L3035**
L3040, and L5100	**East-West**	**L3045**
L3170, and 5260	**East-West**	**L3175**
L3180, L5280, and L5290	**East-West**	**L3185**
L3190, L5320, and L5330	**East-West**	**L3195**
L3200, L5360, and L5370	**East-West**	**L3205**
L3210, L5390, and L5420	**East-West**	**L3215**
L3220, and L5440	**East-West**	**L3225**
L3230, and L5460	**East-West**	**L3232**
L3240, and L5490	**East-West**	**L3245**
L3250, and L5520	**East-West**	**L3255**
L3260, and L5550	**East-West**	**L3265**
L3270, and L5570	**East-West**	**L3275**
L3280, and L5590	**East-West**	**L3285**
L5000, and L5010	**East-West**	**L5005**
L5050, and L5060	**East-West**	**L5055**
L5080, and L5090	**East-West**	**L5085**
L5200, and L5210	**East-West**	**L5205**
L5300, and L5310	**East-West**	**L5305**
L5340, and L5350	**East-West**	**L5345**
L5410, and L5430	**East-West**	**L5415**
L5510, and L5530	**East-West**	**L5515**

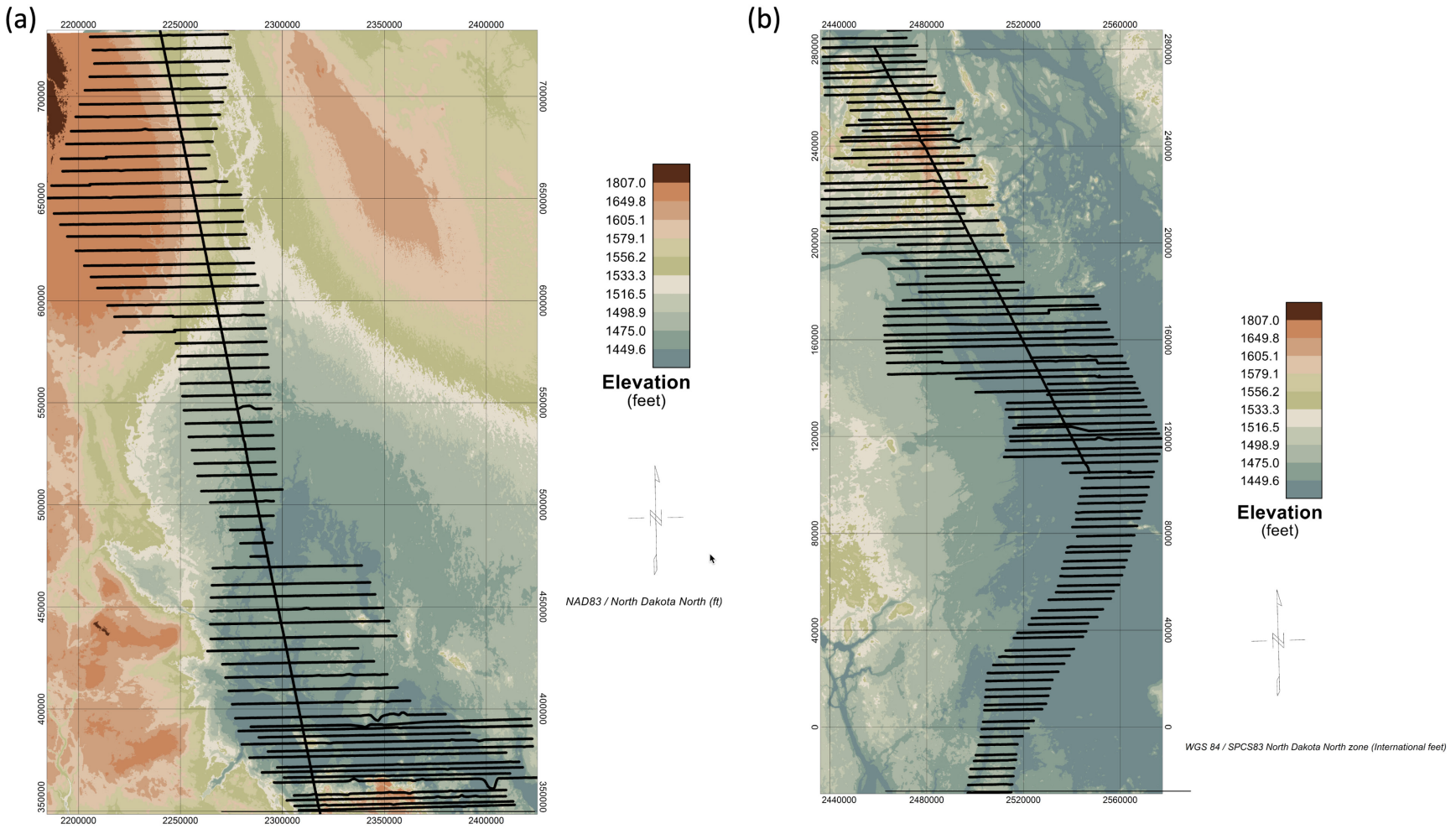

Figure 7-1. (a) Digital elevation model (DEM) of the NDSWC Towner Block AEM survey area. Flight Lines are indicated by black lines. (b) Digital elevation model (DEM) of the NDSWC Griggs Block AEM survey area. Flight Lines are indicated by black lines.

7.3 Display of the AEM Inversions in 2D and 3D

Two-dimensional (2D) and three-dimensional (3D) images of the SCI inversion results have been developed using Datamine Discover PA (DatamineDiscover, 2020). An example 2D-profile for line L1340 from the Towner Block is presented in Figure 7-2. Each profile has a unique length and the profiles are fitted to the size of the profile page. Each profile has a small index map on the upper right showing the location of the survey flight lines with the red line indicating the current profile being displayed. On the upper left is a flight path 2D map of the displayed profile on a background map of the U.S. Geological Survey 100K Topo Map series (USGS, 2019). The horizontal scale of the flight path map is exactly the same as the profile. The lower profile is the AEM SCI inverted resistivity (ohm-m) profile along with the lithology of a borehole if the borehole is within 1/4 mile or 1,320 feet of the flight line. The color scale is in log-space and stretches from 5 to 50 ohm-m (pink to blue). The vertical exaggeration is set high to allow inspection of the details of the inversions. It is important to note that the vertical exaggeration will change with the changing profile length. Appendix 1 contains all the flight line 2D profiles in this full format as well as a simplified format without the inset maps nor the explanation text.

The gray dashed lines, when visible, are the bounds of the upper and lower depth of investigation (DOI). The DOI provides a general estimate of the depth to which the AEM data are sensitive to changes in the resistivity distribution at depth (Christiansen and Auken, 2012). Two DOI's are calculated: an "Upper" DOI at a cumulative sensitivity of 1.2 and a "Lower" DOI set at a cumulative sensitivity of 0.6. A more detailed discussion on the DOI can be found in Asch et al. (2015). Figure 7-3 is a map view of the lower and upper DOI's for the Towner Block AEM survey area and Figure 7-4 is a map view of the lower and upper DOI's for the Griggs Block AEM survey area. The DOI reflects the bandwidth of the system, resistivity of the area, the system/ambient noise, and altitude of the sensor. Typically, in areas of more resistive materials the DOI is greater. For this reason, the DOI plots will reflect the basic geology of the area including deeper DOI's in the areas of the sand and gravel deposits.

3D Fence Diagrams were constructed using a vertical exaggeration of 1:20 of the geolocated profiles using the same 5-50 ohm-m log color scale used in the 2D Profiles. Figure 7-5 is a 3D fence diagram example of the Towner Block AEM survey area looking toward the northeast. Several of the paleochannel systems in the southern part of the Towner block can be seen in this view blue high resistivity sand and gravels. Figure 7-6 is an 3D fence diagram example of the Griggs Block AEM survey area looking north. Much of the paleochannel system can be seen in this view as the blue high resistivity sand and gravels. It is important to note that the resistivity correlates between lines and that there are no sharp breaks in the resistivities over the area of the survey. This indicates good calibration and consistent system performance. A series of images of the 3D fence diagrams for both the Towner and Griggs Blocks are contained within Appendix 2 – 3D Images.

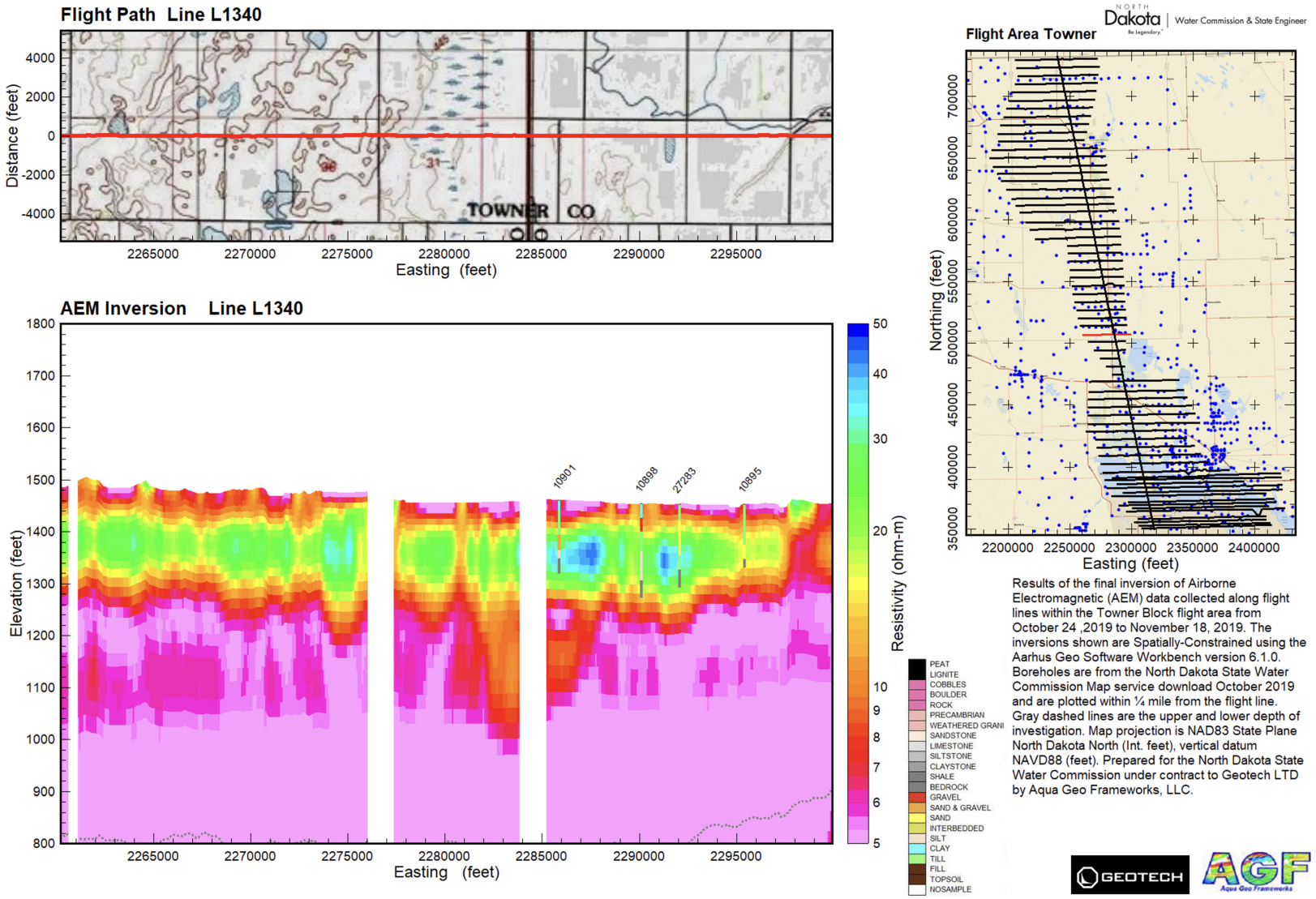

Figure 7-2. Example 2D profile displaying the results of the SCI inversion of NDSWC Towner Block AEM survey flight line L1340 including NDSWC borehole lithologies within ¼ mile (1,320 feet) of the flight line. The resistivity color scale is on the right side of the profile.

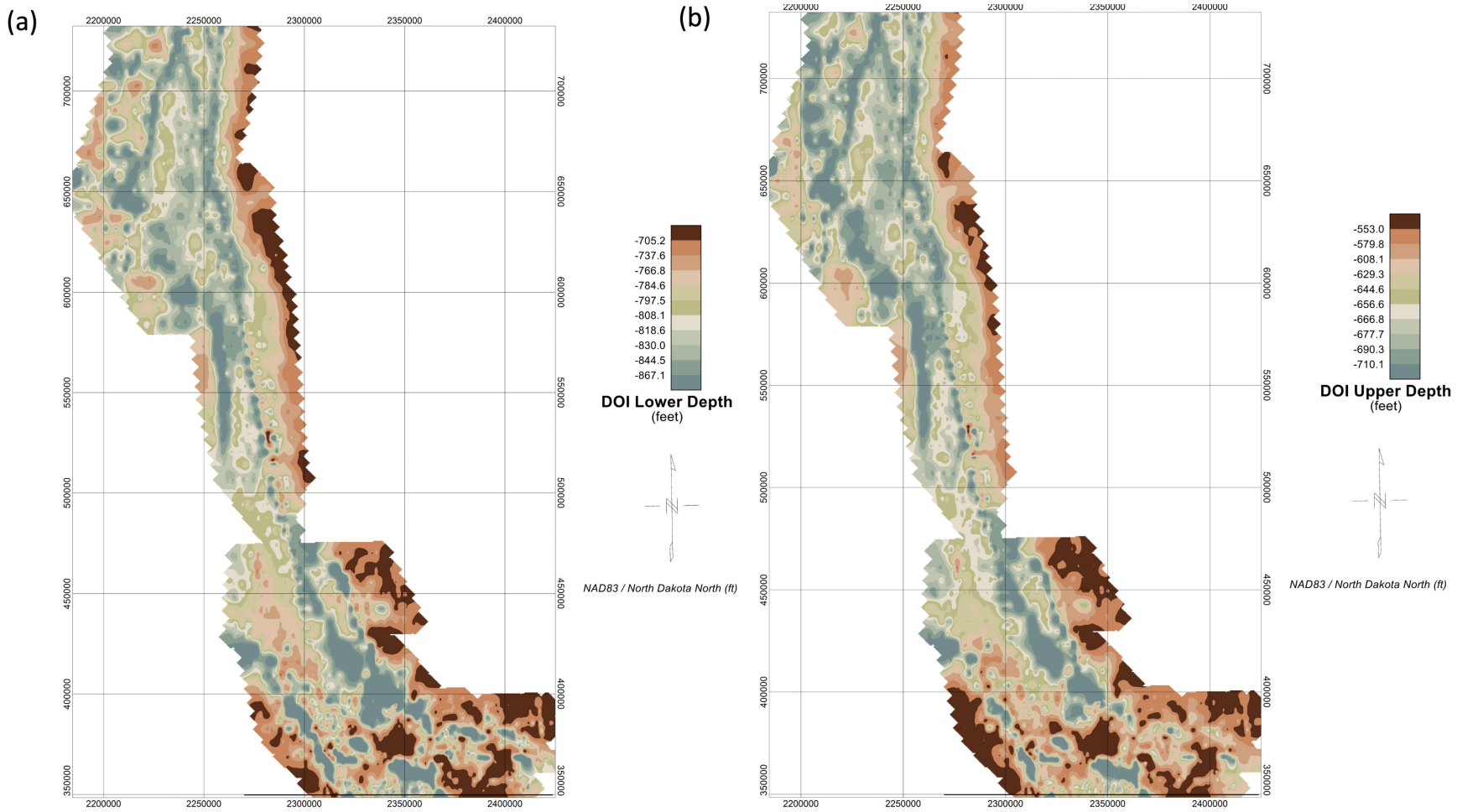

Figure 7-3. The (a) Lower and (b) Upper Depth of Investigation (DOI) of the Towner Block AEM Spatially-Constrained Inversion (SCI). Flight lines are indicated by black lines. Note that each image has its own color scale in depth which is different from the other images.

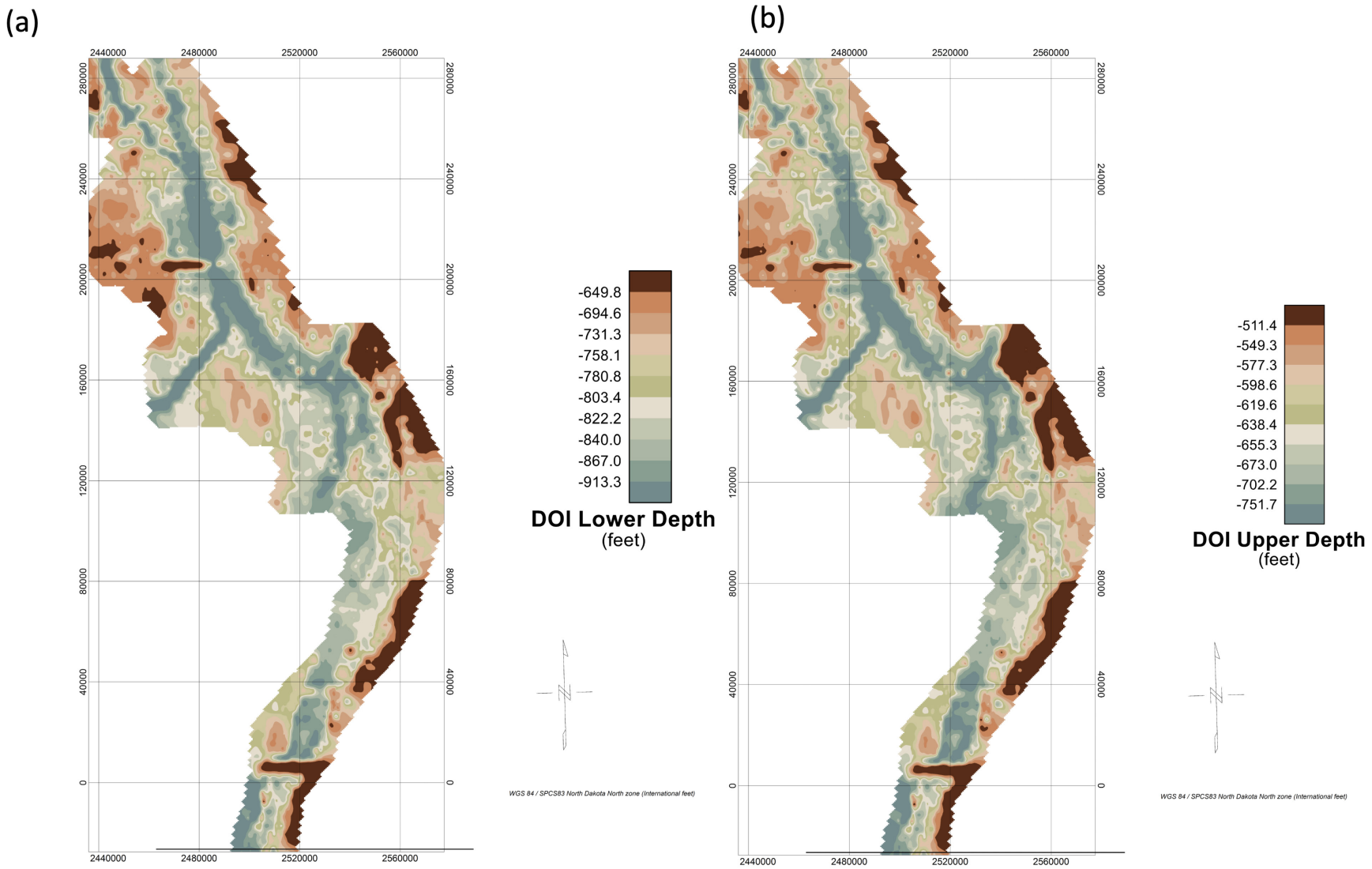

Figure 7-4. The (a) Lower and (b) Upper Depth of Investigation (DOI) of the Griggs Block AEM Spatially-Constrained Inversion (SCI). Flight lines are indicated by black lines. Note that each image has its own color scale in depth which is different from the other images.

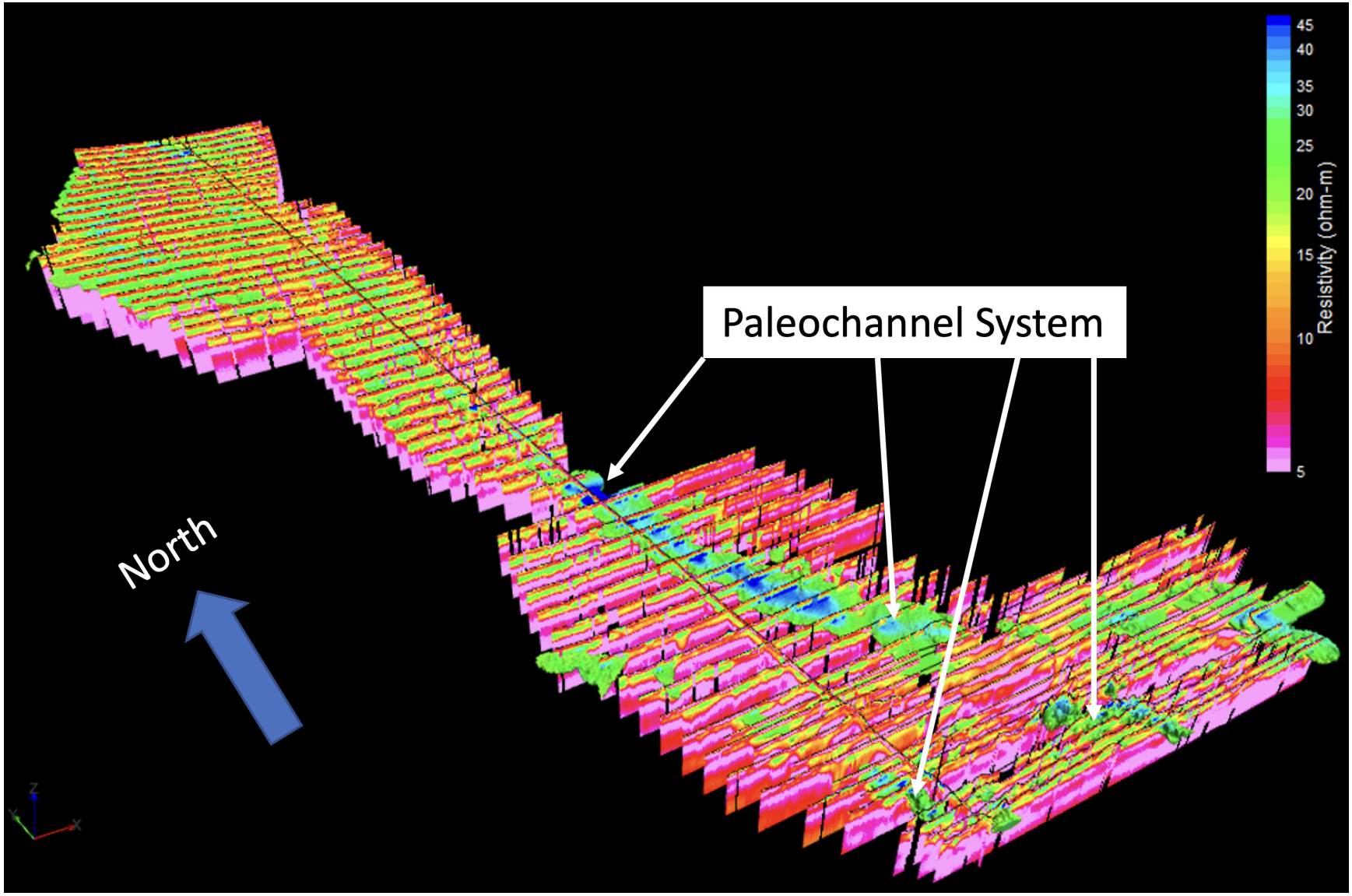

Figure 7-5. Example 3D fence diagram displaying the results of the Towner Block AEM survey. The color scale is from 5-50 ohm-m, log-based. The view is to the northeast. Vertical Exaggeration 20x.

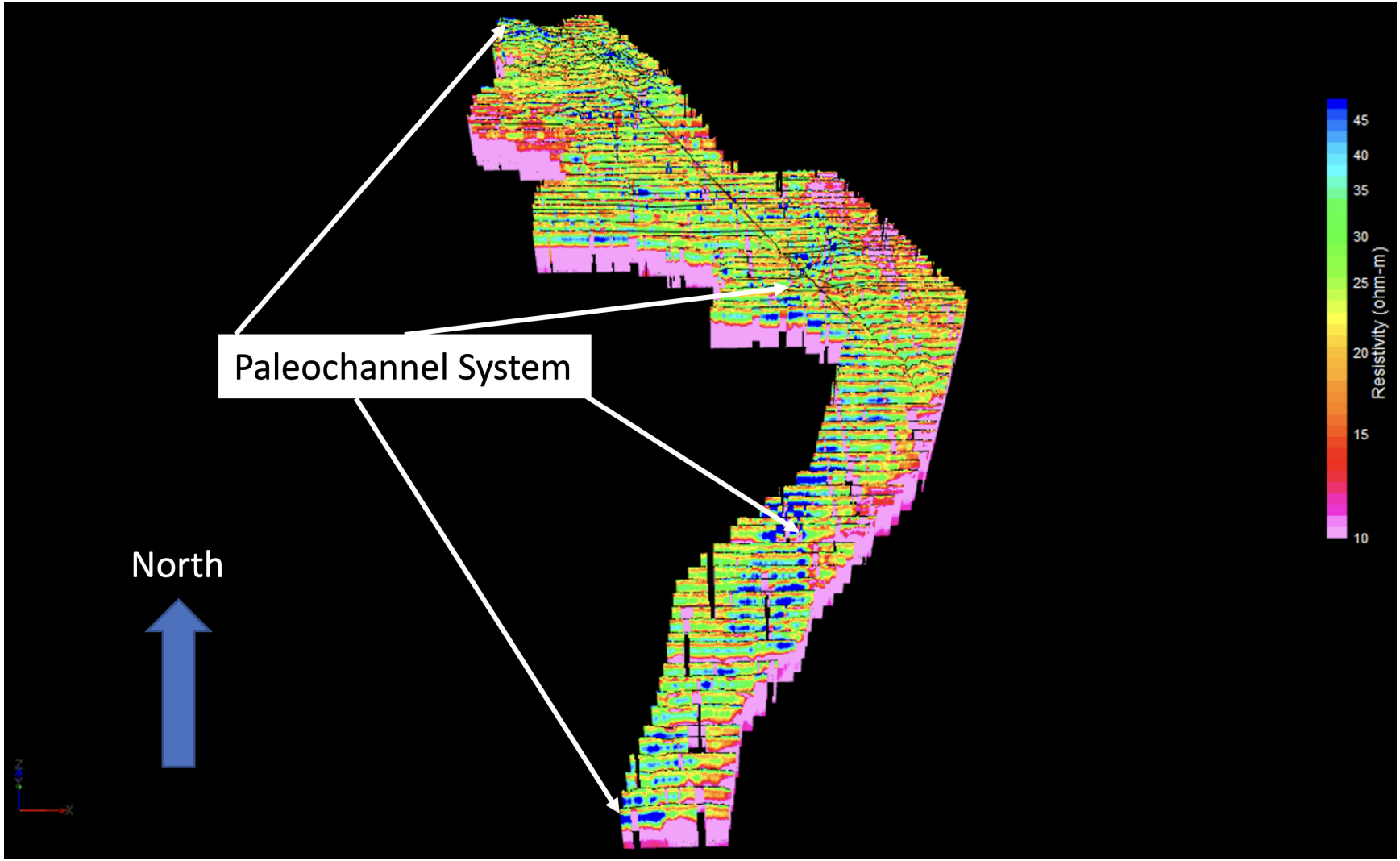

Figure 7-6. Example 3D fence diagram displaying the results of the Griggs Block AEM survey. The color scale is from 5-50 ohm-m, log-based. The view is to the north. Vertical Exaggeration 20x.

7.4 Resistivity Depth Layers

Resistivity depth layers were created based on the SCI model cell spacing (Table 5-1) and were used to produce resistivity layer plots of the both the Towner and Griggs Block AEM survey areas. To create these grids, the resistivities of the individual model layers were imported to a Geosoft Oasis montaj (OM) database. The individual model layers were then gridded independently using the OM Minimum Curvature Gridding (MCG) algorithm. The cell size was set to 500 feet, a blanking distance of 500 feet was applied, and the "cells to extend beyond" set to 3 or 1,500 feet. All other parameters were either left as the default or blank. These layers are useful for inspecting the vertical changes in the resistivity. The color scale that was used for these maps was selected to illuminate the sands and gravels within the Quaternary section. Figure 7-7 is an example of a model depth layer 15, from -190 ft to -208.9 ft from the Towner Block AEM survey area. At this depth the basic fabric of the Quaternary sands and gravels are indicated by the high resistivities (blue). For this layer the color scale is automatically stretched to cover the range in resistivity using a histogram distribution. Figure 7-8 is an example of a model depth layer 18, from –249.5 to -271.3 ft from the Griggs Block AEM survey area. The color range is the same as used in the profiles and fence diagrams - a log distribution from 5 to 50 ohm-m. In this example the sands and gravels are also indicated by the high resistivities (green-blue). A set of images with the log distribution 5 to 50 ohm-m color scale and the auto range per layer histogram distribution color scale was made. The 5 to 50 ohm-m color scale will be consistent through the profiles and 3D fence diagrams while the histogram stretched color scale will allow inspection of subtle details in each layer. It is important to note that the auto scaled histogram color scales cannot be directly compared to the profiles nor different layers. These layers have been combined into both PDF files and Google Earth KMZ's that allows the user to inspect the individual layers by selecting a specific layer under the Data tab in the layered pdf files which are located in *Appendix 3 – Deliverables*\ *PDF*. The grids of these layers can be found in *Appendix 3 – Deliverables**Grids* as well as layered KMZ's in *Appendix 3 – Deliverables**KMZ*.

7.5 Voxel Grid

Voxel grids were developed for the Towner and Griggs Block AEM survey areas. The voxel grids were made using a 500ft grid cell size and the model layer thicknesses (Table 5-1). A minimum curvature method was used within Datamine Discover PA (Datamine Discover, 2020). The grid was allowed to interpolate to the extents of the survey with some areas of no data coverage due to EM coupling clipped from the grids. All layers were referenced to their depth from the surface. After the grid was calculated, the DEM was added as an offset.

The voxels allow for another view with which inspection of the 3D distribution of the inverted model resistivities can be made. Specifically, for the inspection of the Towner Block AEM survey the paleochannel deposits can be highlighted using a 25 ohm-m threshold. Figure 7-9 is a 3D Fence Diagram plot of the AEM resistivities with a >25 ohm-m resistivity threshold on the voxel for the Towner Block AEM survey area looking at the southern portion of the Block from the southeast toward the northwest. The paleochannel deposits (green-blue) are visible amongst the low resistivity clays and shale (red-pink). Figure 7-10 presents a 3D plot of a voxel with a >35 ohm-m threshold for the Griggs Block AEM survey area with the 3D Fence Diagrams looking from the east toward the west. The paleochannel deposits (blue) are visible amongst the low resistivity clays and shale (red-pink).

The complete collection of the 2D profiles are contained in *Appendix 1* and the images of the3D Fence Diagrams, resistivity depth layers, and voxels, are contained in *Appendix 2*. Layered PDF's of resistivities of model layers can be found in *Appendix 3 – Deliverables\PDF* and as are ArcView Binary Raster Grids. The voxel may be found in *Appendix 3 – Deliverables\Voxel* as an ASCII *.xyz.

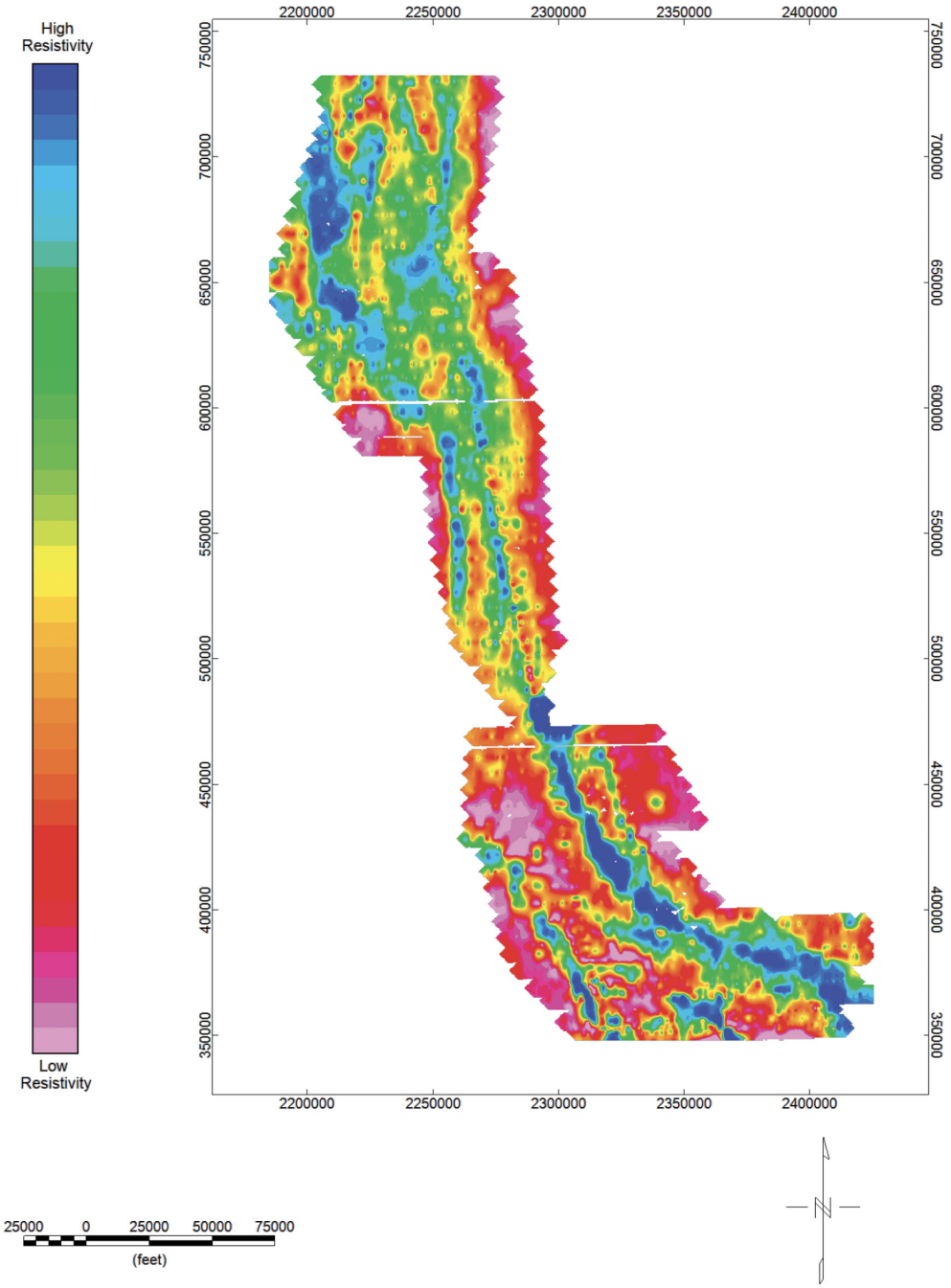

Figure 7-7. Map view of the inverted AEM resistivity for the 15th SCI model layer from –190 ft to –208.9 ft feet for the Towner Block AEM survey area. The color scale is an automatic scaled histogram distribution.

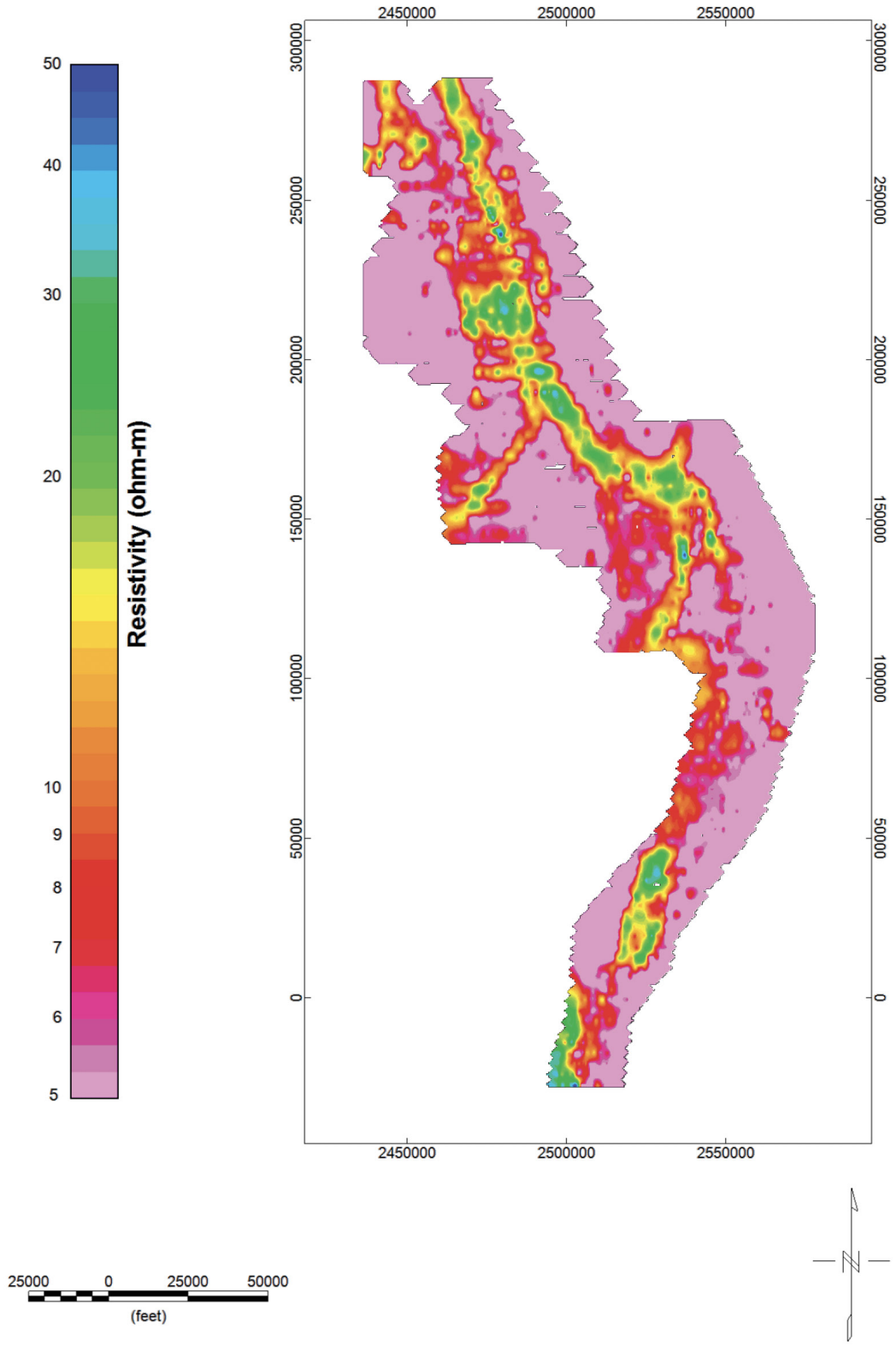

Figure 7-8. Map view of the inverted resistivity for the 18th SCI model layer –249.5 to –271.3 ft for the Griggs Block AEM survey area. The color scale is log distribution from 5 to 50 ohm-m.

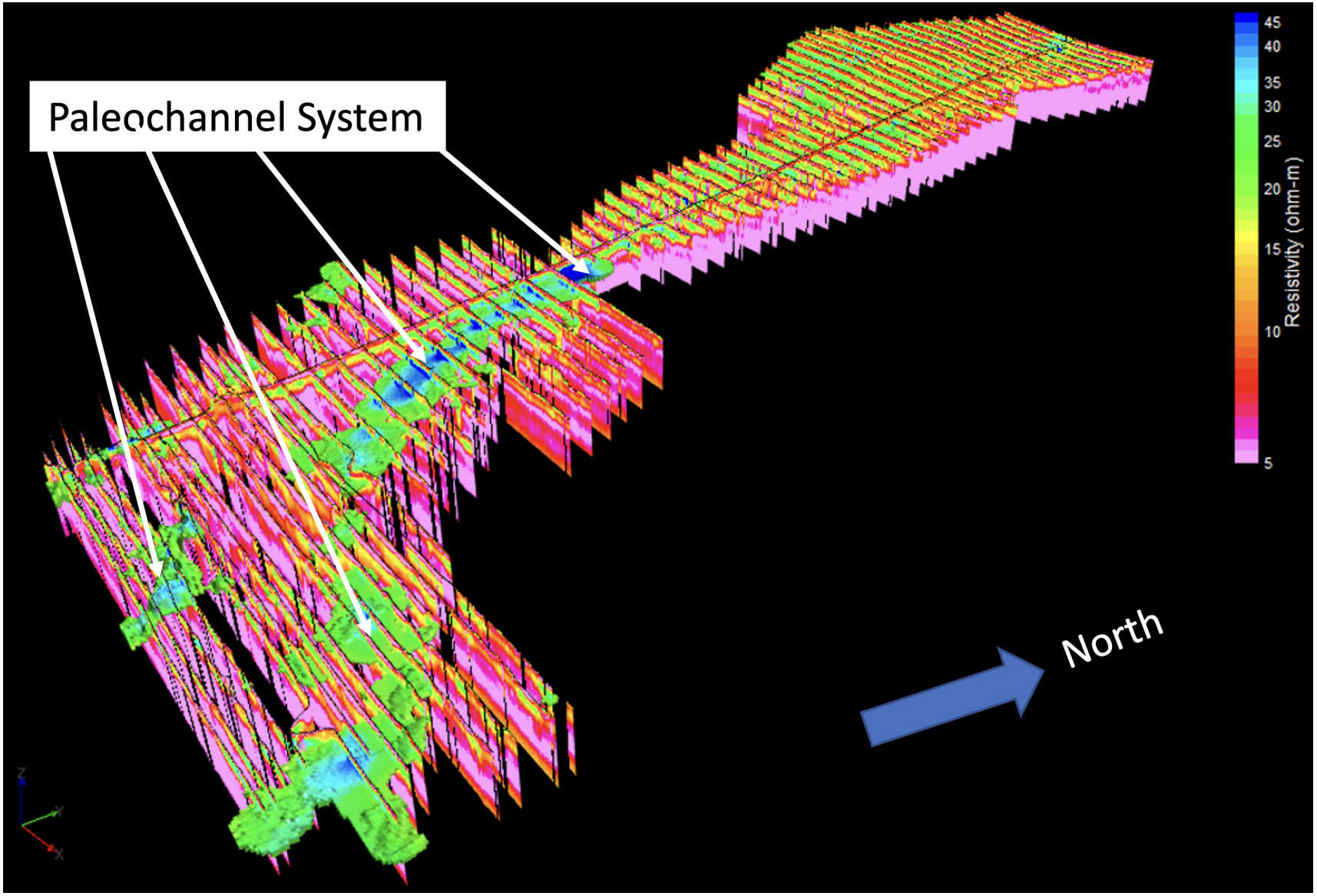

Figure 7-9. 3D image of a >25 ohm-m voxel and 3D fence diagrams of the Towner Block AEM survey area. The view is looking from the southeast toward the northwest. Vertical Exaggeration is 20x.

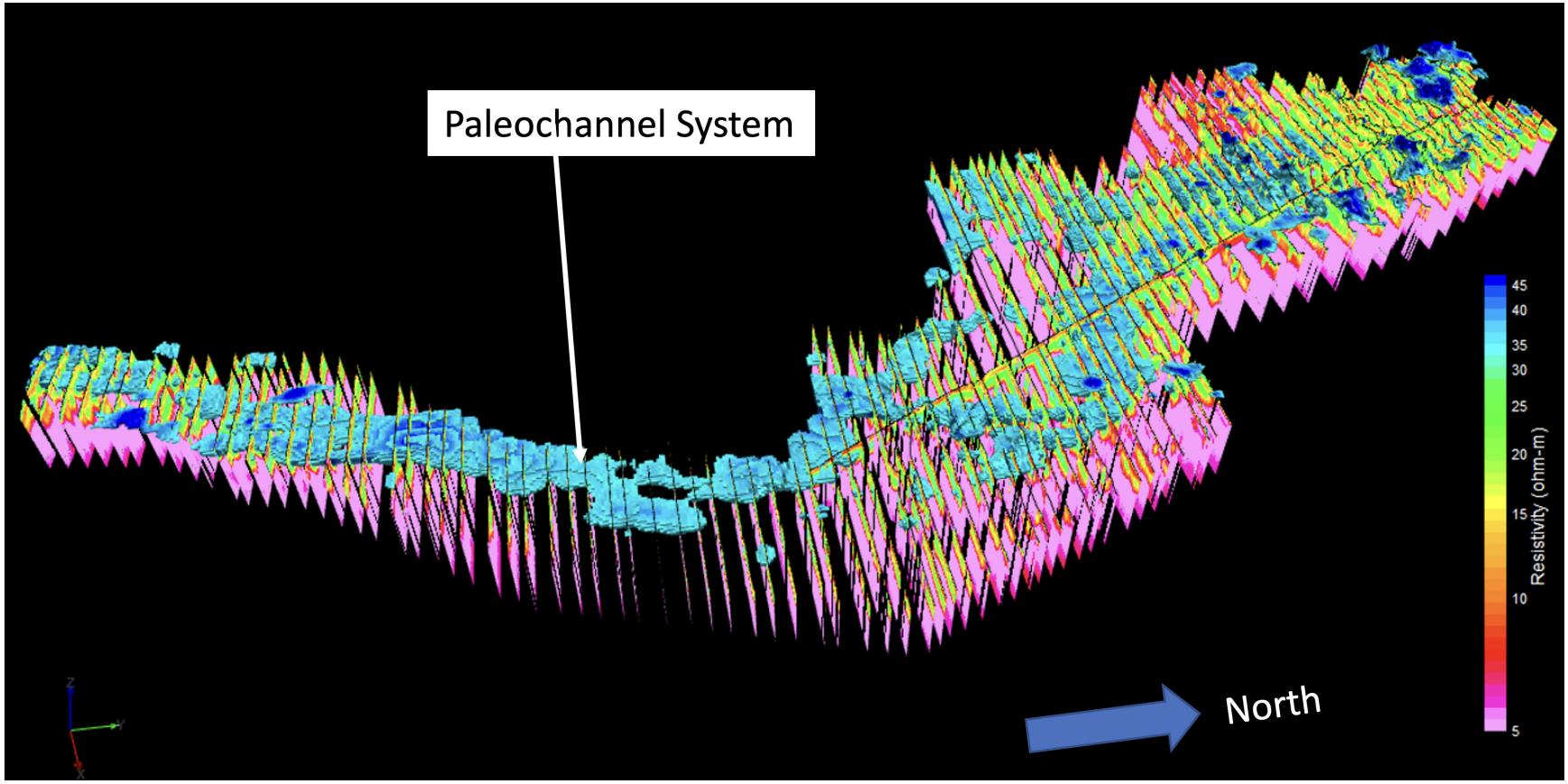

Figure 7-10. 3D image of a >35 ohm-m voxel and 3D fence diagrams of the Griggs Block AEM survey area. The view is looking from the east toward the west. Vertical Exaggeration is 20x.

7.6 Resistivity Elevation Layers

Resistivity elevation layers were created based on the voxel model in order to assist in the visualization of the resistivity variations related to the elevations of the deposits. To create these grids, the voxel model was sampled at discrete elevation ranges and the resulting resistivities were gridded at a 500 ft cell size. Figure 7-11 is an example of two elevation layers, 1,400 ft and 1,200 ft, from the Towner Block AEM survey area. For Figure 7-11 the color scales are automatically stretched to cover the range in resistivity in each layer using a histogram distribution per layer. Thus, the two color scales are not equal, but emphasize the details per layer. Figure 7-12 presents two examples of resistivities at elevations 1,400 ft and 1,200 ft of the Griggs Block AEM survey area. These two layers show the changes in the deposits with elevation and are at the same color scale of 5 to 50 Ohm-m with a log distribution.

All the elevation layers for both the Towner and the Griggs Blocks were combined into two different PDF files and Google Earth KMZ's for the two different color scales that allows the user to inspect the individual layers by selecting a specific layer under the Data tab in the pdf file. These files are located in *Appendix 3 – Deliverables**PDF*. The grids of these layers can be found in *Appendix 3 Deliverables**Grids*.

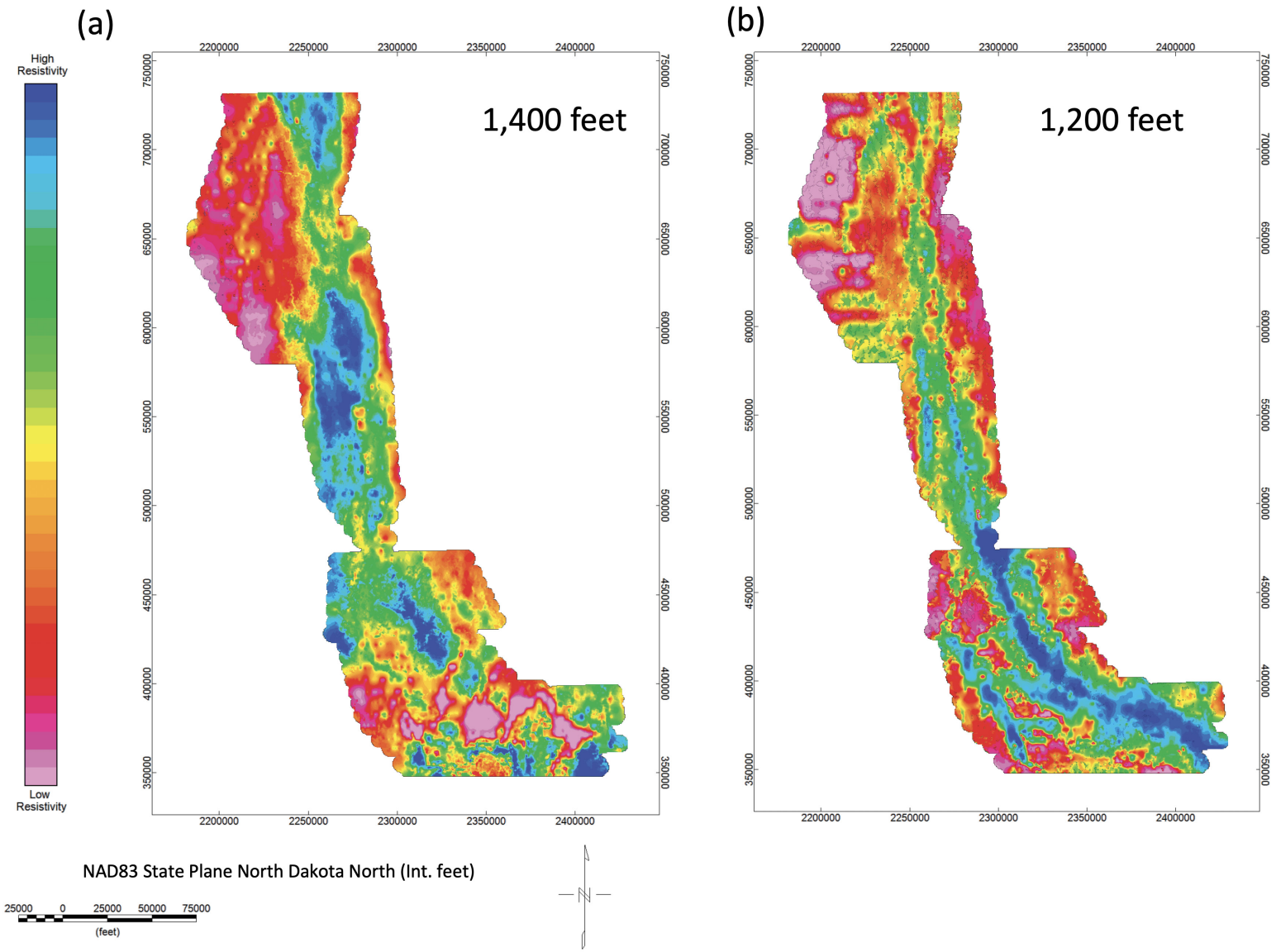

Figure 7-11. (a) Resistivity layer at an elevation of 1,400 ft of the Towner Block AEM survey area (b) Resistivity layer at an elevation of 1,200 ft of the Towner Block AEM survey area. The color scale is an automatic scaled histogram distribution for each layer.

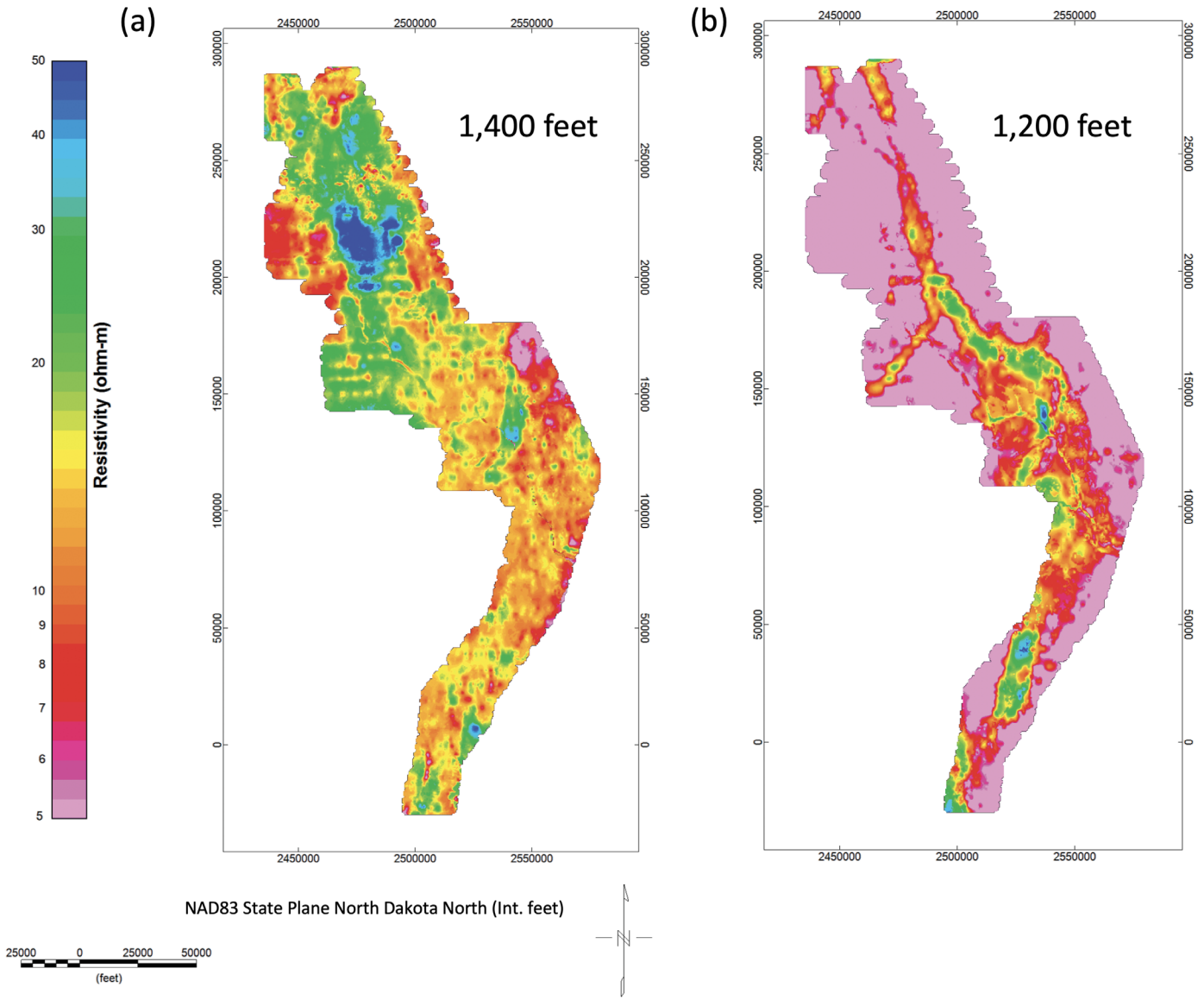

Figure 7-12. (a) Resistivity layer at an elevation of 1,400 ft of the Griggs Block AEM survey area (b) Resistivity layer at an elevation of 1,200 ft of the Griggs Block AEM survey area. The color scale is log distribution from 5 to 50 ohm-m.

7.7 Examples of Boreholes Electrical Resistivity and Lithology Compared to AEM Inversion

Two borehole databases were downloaded from the NDSWC website. One was the Test Hole database and the other was the Observation Well database (NDSWC, 2019). The databases contained information on the interpreted lithology from well drilling and were examined within the area. Only the NDSWC-owned boreholes were used in this project. Edits were conducted on the database to correct typo's or inconsistencies in the lithology descriptions. The lithologies were examined and the color scale for the display of the lithologies was provided by the NDSWC (Personal Communications, Scott Parkin, Hydrologist, and Rex Honeyman, Hydrologist NDSWC, November 2, 2017).

Six modern electrical resistivity logs were also provided for the survey area holes (Personal Communications, Rex Honeyman, Hydrologist NDSWC, October 16, 2019). One of the logs is within the Towner Block and four logs are in the Griggs Block (Figure 7-13). As indicated in Section 7.3, 2D profiles, boreholes that were within ¼ of a mile or 1,320 feet of the flight line, were projected onto the AEM inverted resistivity profiles. Several observations have been noted below that will hopefully assist the NDSWC in the interpretation of the AEM inverted resistivities including pointing out some areas of good correlation with the borehole lithology as well as areas of poor correlation of the borehole lithology to the inverted AEM resistivity. It is of paramount importance that the interpreter understands the limitation of the lithology descriptions as compared to the resistivity as well as understand the limitations of the AEM.

An AEM system is responding to changes in the electrical resistivity of the subsurface while flying at approximately 50 mph at approximately 100 ft above ground level (AGL) with a finite EM bandwidth. This means that it is possible that the AEM could provide a fuzzy or unfocused view of the subsurface as compared to borehole lithology or borehole geophysics. As the EM signal diffuses down into the earth, the amplitude of the signals returned to the receiver on the AEM platform have detectable decreases. This has the impact of decreasing the resolution of the EM signals with increasing depth. The AEM inversion models also increase layer thickness with depth that also express the possible decreased resolution of the technique with depth (Table 5-1).

Lithology logs are also limited by the following: drilling method, drilling mud, drilling speed, and skill and experience of the geologist performing the descriptions. The lithology log is an interpretation by the geologist of the material that is brought to the surface. Different vintages of lithology logs catalogued at differing times by different geologists may have varying accuracies in specific picks of similar lithologies. Cores are an improvement in the interpretation of the lithology over other methods but are also plagued with difficult recovery in unconsolidated materials. With all the limitations of the lithology logging of well cuttings, the fact remains that they are still a window into the subsurface and provide important clues to the geology. Below are several examples of comparisons of boreholes with the AEM inverted resistivities. *Appendix 1 – 2D Profiles* includes these examples and others for comparison of selected flight lines with the borehole lithology logs.

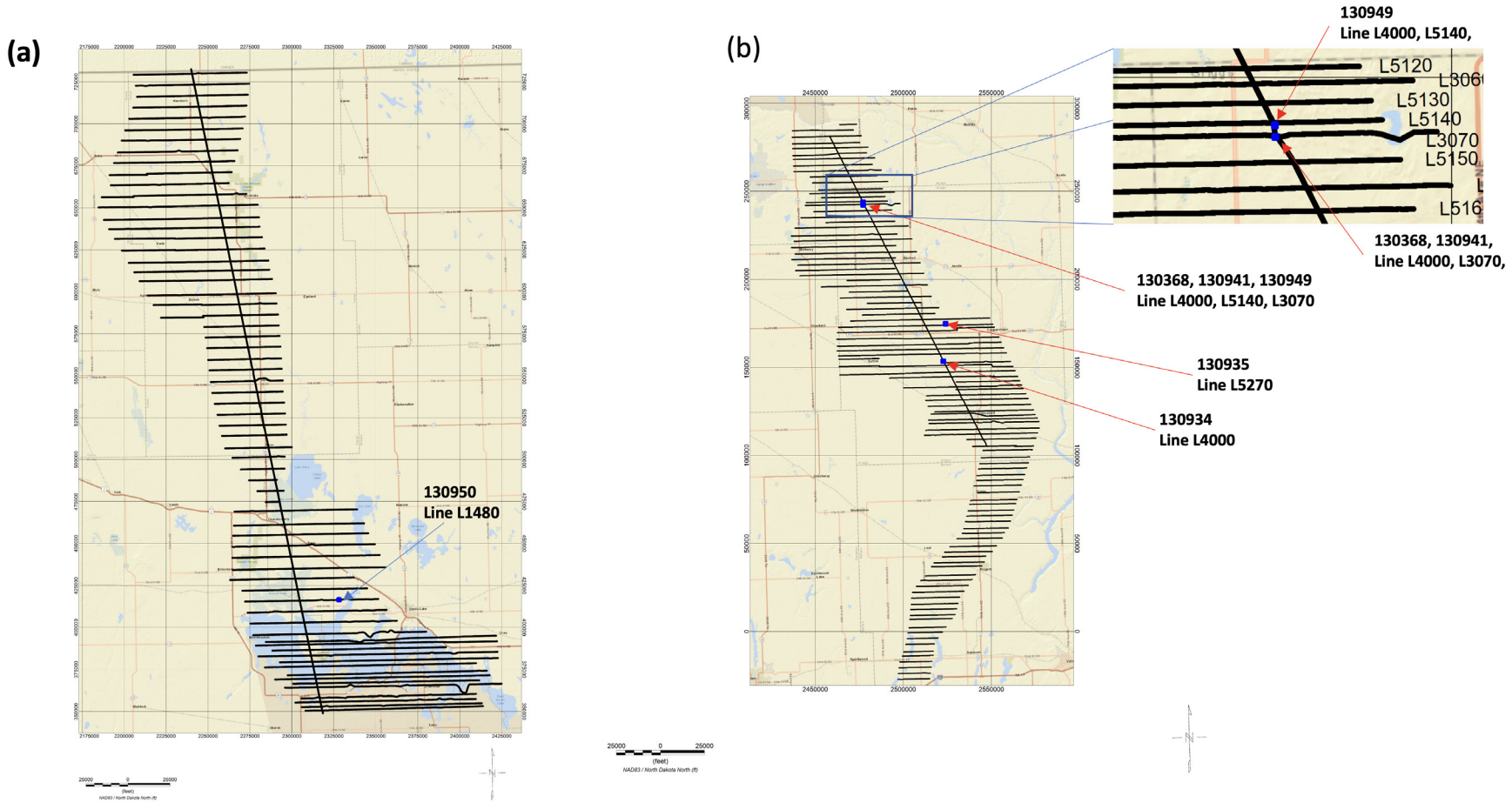

Figure 7-13. Map of the location of the (a) Towner and (b) Griggs E-logs on the flight lines.

7.7.1 E-Log Comparisons to AEM

The 16-inch normal and the 64-inch normal resistivity logs were used by Geotech LTD to calibrate the AEM data. Several lines were flown over the test holes to be used in the calibration. Two holes are very close to one another, *130941* and *130368* (Table 7-3).

Table 7-3. Test lines with E-log test holes.

Flight Lines	Test hole	Area
L1480	**130950**	**Towner Block**
L4000, L5140	**130949**	**Griggs Block**
L4000, L3070	**130941**	**Griggs Block**
L4000, L3070	**130368**	**Griggs Block**
L5270	**130935**	**Griggs Block**
L4000	**130934**	**Griggs Block**

Figure 7-14 is a comparison of the SCI inversions of line L1480 flown over test hole *130950* for both the 16-inch Short Normal and 64-inch Long Normal in the Towner Block AEM survey area. The 16-inch Short Normal and the 64-inch Long Normal logs present quite similar resistivities indicating that there is limited lateral variation on the order of the 64 inches around the borehole. There is a slight increase in the resistivity in the 16-inch as compared to the 64-inch within the resistive zone but that is minor. The AEM and the E-logs corelate well at the top of the resistive materials at ~ 1,370 feet as the resistivities match well. The E-log also indicates the bottom of the resistive materials ending at a low resistivity unit at ~1,290 feet. The AEM indicates a lower resistivity material as compared to the E-log, but this is in an area of EM-coupling that has been removed. At the very top of the 64-inch there appears to be some interference from the air-filled borehole indicated by a resistive zone.

Figure 7-15 is a comparison of the SCI inversions of line L5270 flown over test hole *130935* for both the 16-inch Short Normal and 64-inch Long Normal in the Griggs Block AEM survey area. The 16-inch Short Normal and the 64-inch Long Normal logs are similar indicating low spatial variation. However, both show that the air-filled borehole at the top caused increased resistivity. The E-logs and the AEM show that the area is between 18-30 ohm-m and both the E-logs and the AEM show low resistivity materials at ~ 1245 feet.

Figure 7-16 is a comparison of the SCI inversions of line L4000 flown over test hole *130934* for both the 16-inch Short Normal and 64-inch Long Normal in the Griggs Block AEM survey area. The 16-inch Short Normal and the 64-inch Long Normal logs are similar indicating low spatial variation. However, both show that the air-filled borehole at the top caused increased resistivity. The E-logs and the AEM show that the area is between 18-30 ohm-m. There is an increase in the resistivity in the 16-inch as compared

to the 64-inch within the resistive zone below ~1,300 feet. Both the E-logs and the AEM show the low resistivity materials at ~ 1220 feet. There is a low resistivity zone from ~1,350 to ~1,300 feet that is indicated in the E-logs but is not indicated in the AEM inversion results as this borehole is located in a region where the EM-coupling was removed from the AEM data and we can't know if that low resistivity zone is there or not in the inversion results.

Figure 7-17 is a comparison of the SCI inversions of line L4000 flown over test hole *130941* and *130949* for both the 16-inch Short Normal and 64-inch Long Normal for the Griggs Block AEM survey area. The 16-inch Short-Normal and the 64-inch Long-Normal logs are similar but not exactly the same in resistivity, indicating that there is some lateral variation on the order of the 64 inches around the borehole. However, both show that the air-filled borehole at the top caused increase resistivity. The AEM has a large coupling in the area of the *130941*, but is matching well with the exception of the bottom of the E-log. This may be related to some EM coupling that was not fully removed from the data at that location. Test hole *130949* doesn't match the AEM that well with the exception of the low resistivity unit at ~1,300 to ~1,200 feet. The AEM under-predicts the resistivity from ~1,500 to ~1,350, but does indicate a higher resistivity zone. The deeper E-log resistivity zone in *130940* from ~1,200 to ~1,160 is higher in resistivity as compared to the AEM. This is most likely related to the averaging impact of the AEM signals with depth and the lower resolution of resistive zones as compared with conductors. The AEM does indicate that there is a higher resistivity zone at depth but doesn't fully resolve the true resistivity.

Figure 7-18 is a comparison of the SCI inversions of line L4000 flown over test hole *130368* and *130949* for both the 16-inch Short Normal and the 64-inch Long Normal for the Griggs Block AEM survey area. The 16-inch Short-Normal and the 64-inch Long-Normal logs are similar but not exactly the same in resistivity, indicating that there is some lateral variation on the order of the 64 inches around the borehole. However, both show that the air-filled borehole at the top caused increase resistivity. The AEM has a large coupling in the area of the *130368*, as was discussed above related to hole *130941*. The coupling in this area looks to have masked the lower paleochannels within the section that hole *130368* is indicating. Test hole *130949* was discussed above. Test hole *130368* E-log does corelate well with the low resistivity zone from the AEM at ~ 1,150 feet. Again, there is likely a pull up in the resistivity related to the EM-coupling.

Figure 7-19 is a comparison of the SCI inversions of line L5140 flown over test hole *130949* for both the 16-inch Short Normal and 64-inch Long Normal for the Griggs Block AEM survey area. The 16-inch Short-Normal and the 64-inch Long-Normal logs are similar but not exactly the same in resistivity, indicating that there is some lateral variation on the order of the 64 inches around the borehole. However, both show that the air-filled borehole at the top caused increase resistivity. The AEM comparison is very similar to the comparison of L4000 to test hole *130949*. Overall, there is a good indication of the lower paleochannel at ~ 1,150 to 1,230 feet, but the magnitude of the resistivity is not well resolved in the AEM as compared with the E-log.

Figure 7-20 is a comparison of the SCI inversions of line L3070 flown over test hole *130941* for both the 16-inch Short Normal and 64-inch Long Normal for the Griggs Block AEM survey area. The 16-inch Short-Normal and the 64-inch Long-Normal logs are similar indicating that there is little lateral variation on the

order of the 64 inches around the borehole. However, both show that the air-filled borehole at the top caused increase resistivity. Overall, the comparisons to the AEM is good until the bottom of the E-log. As discussed above this may be related to the coupling along the flight line. The AEM does indicate an increase in the resistivity from ~1,200-1,300 feet that is likely related to a paleochannel.

Figure 7-21 is a comparison of the SCI inversions of line L3070 flown over test hole *130368* for both the 16-inch Short Normal and the 64-inch Long Normal for the Griggs Block AEM survey area. The 16-inch Short-Normal and the 64-inch Long-Normal logs are similar in resistivity, indicating that there is little lateral variation on the order of the 64 inches around the borehole. The AEM comparison is good from ~1,550 to 1,390 feet but doesn't correlate well below that. It looks like the E-log is reversed in this area. This may be related to the EM-coupling but the root cause in not know. Out of all the E-logs discussed, this is the one with the poorest fit.

The purpose of the above section is to verify that the AEM was calibrated properly and the inversion results indicate that the AEM system utilized for this survey (the VTEM Plus) was clearly calibrated. It is also important to understand the limitation of the AEM in resolving features at increasing depth. These comparisons indicated that the AEM is not able to resolve the absolute resistivity of the thin deeper more resistive material. However, the AEM does indicate that there is a zone of increased resistivity. For this reason alone, a combined borehole and AEM interpretation is required to provide the best framework for the area. The area around some of the EM-coupling and the poor correlation to the E-Logs from test hole *130368* is curious and is not fully understood.

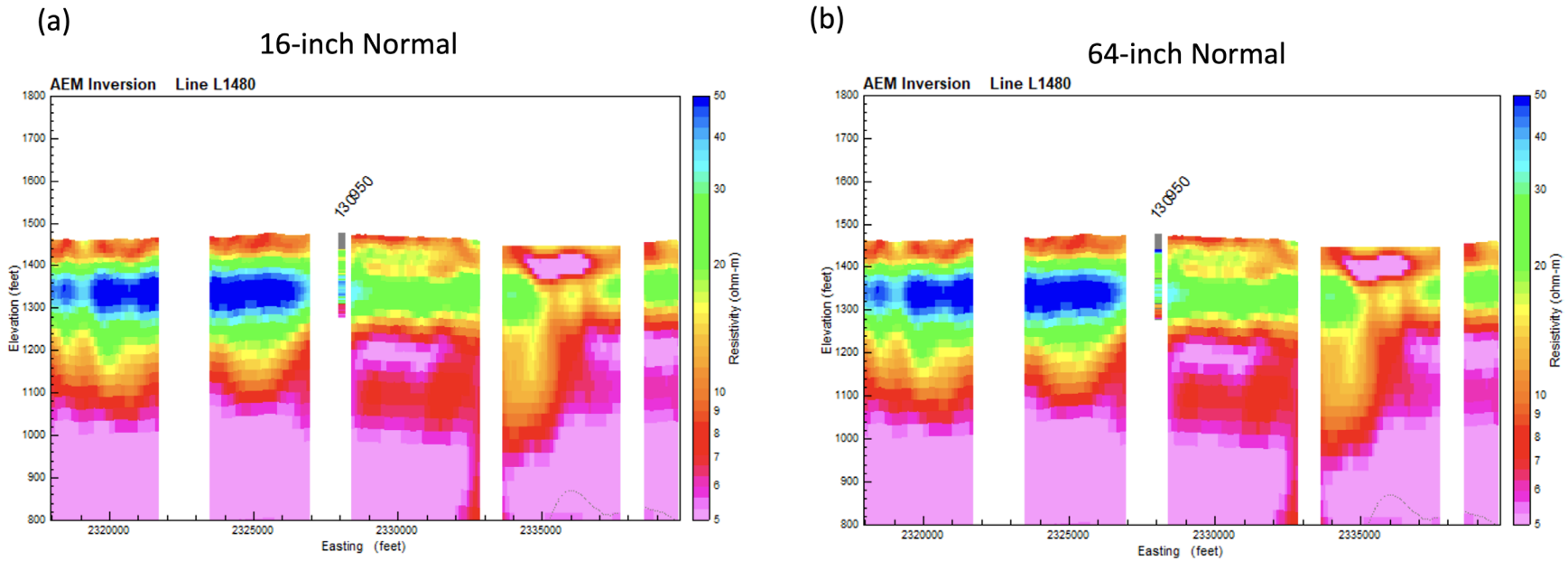

Figure 7-14. A comparison of the SCI inversions of line L1480 flown over test hole *130950* for both the (a) 16-inch Short Normal and (b) 64-inch Long Normal within the Towner Block area.

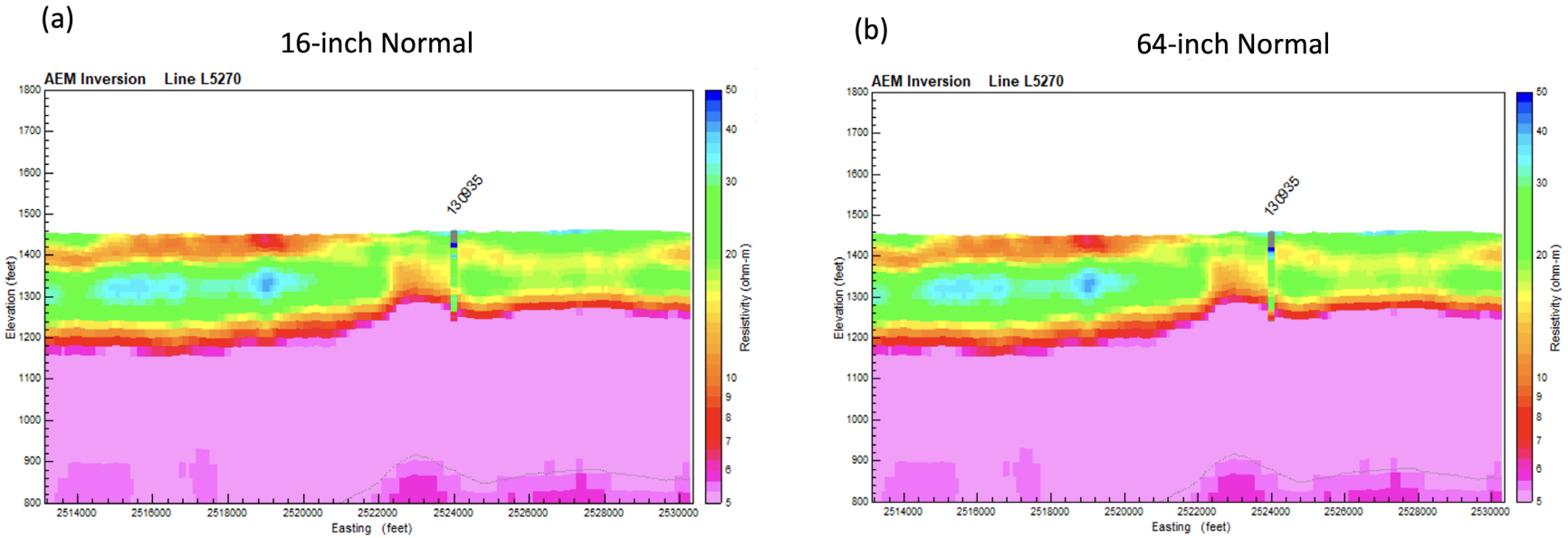

Figure 7-15. A comparison of the SCI inversions of L5270 flown over test hole 130935 for both the (a) 16-inch Short Normal and (b) 64-inch Long Normal within the Griggs Block AEM survey area.

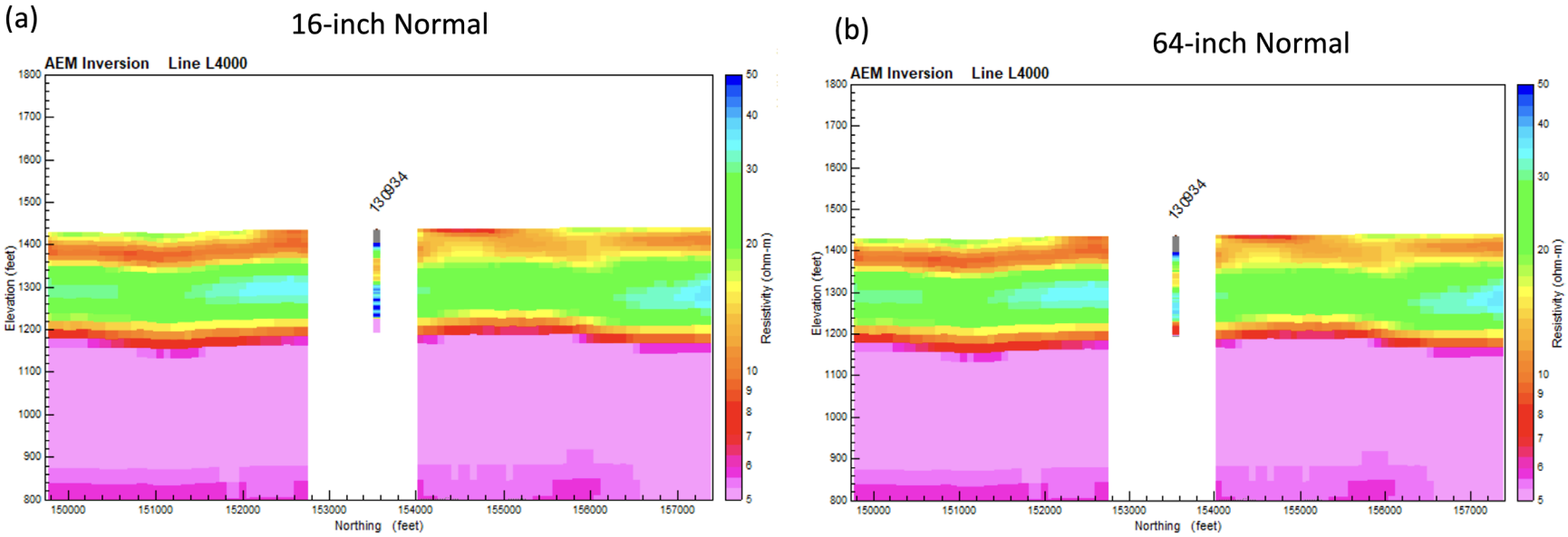

Figure 7-16. A comparison of the SCI inversions of L4000 flown over test hole *130934* for both the (a) 16-inch Short Normal and (b) 64-inch Long Normal within the Griggs Block AEM survey area.

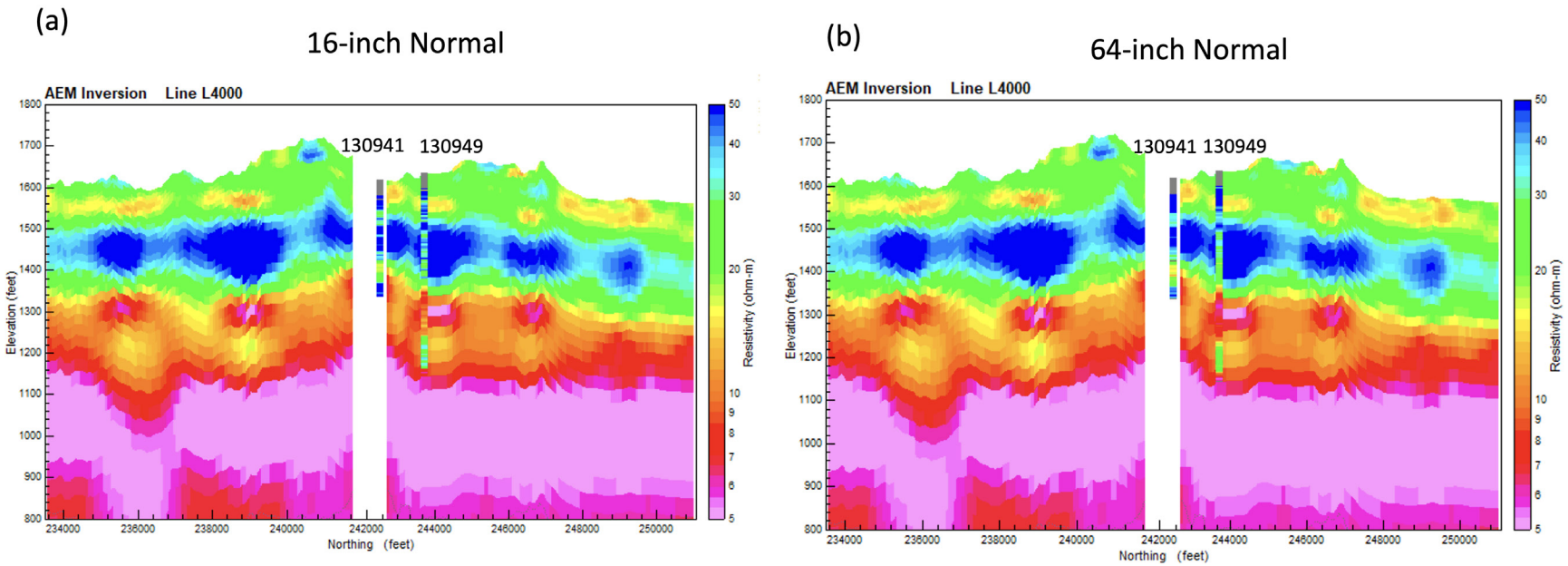

Figure 7-17. A comparison of the SCI inversions of line L4000 flown over test hole *130941* and *130949* for both the (a) 16-inch Short Normal and (b) 64-inch Long Normal within the Griggs Block AEM survey area.

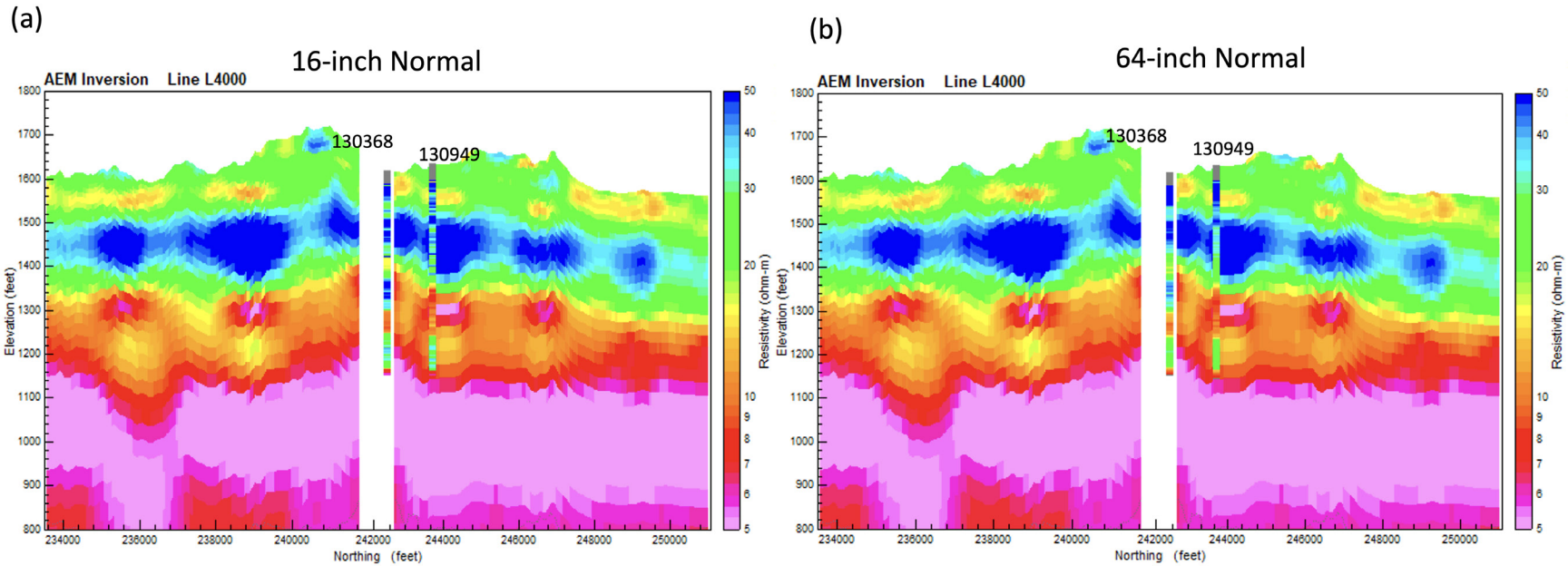

Figure 7-18. A comparison of the SCI inversions of line L4000 flown over test hole *130368* and *130949* for both the (a) 16-inch Short Normal and (b) 64-inch Long Normal within the Griggs Block AEM survey area.

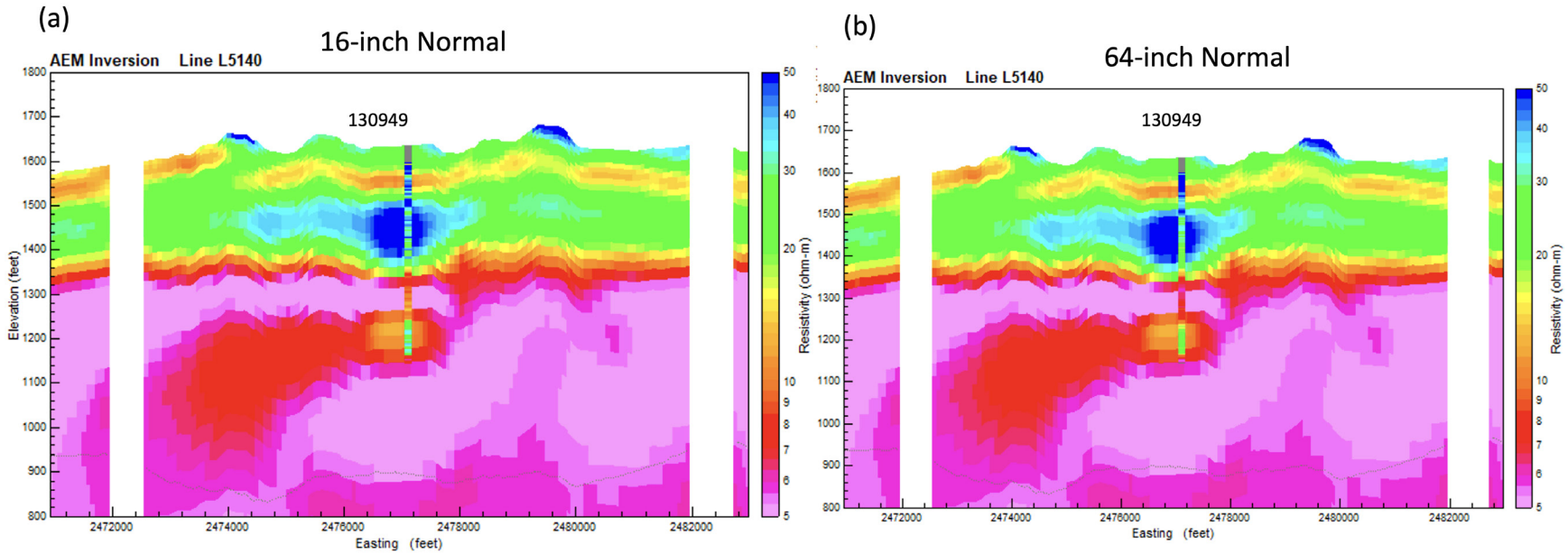

Figure 7-19. A comparison of the SCI inversions of line L5140 flown over test hole *130949* for both the (a) 16-inch Short Normal and (b) 64-inch Long Normal within the Griggs Block AEM survey area.

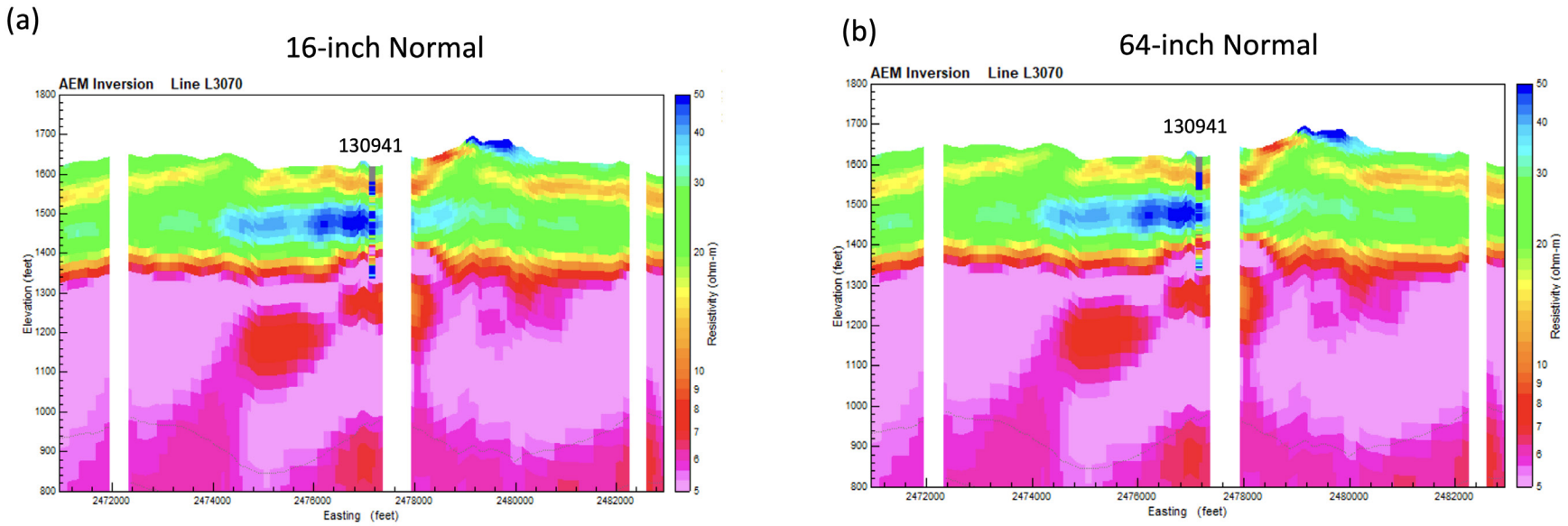

Figure 7-20. A comparison of the SCI inversions of line L3070 flown over test hole *130941* for both the (a) 16-inch Short Normal and (b) 64-inch Long Normal within the Griggs Block AEM survey area.

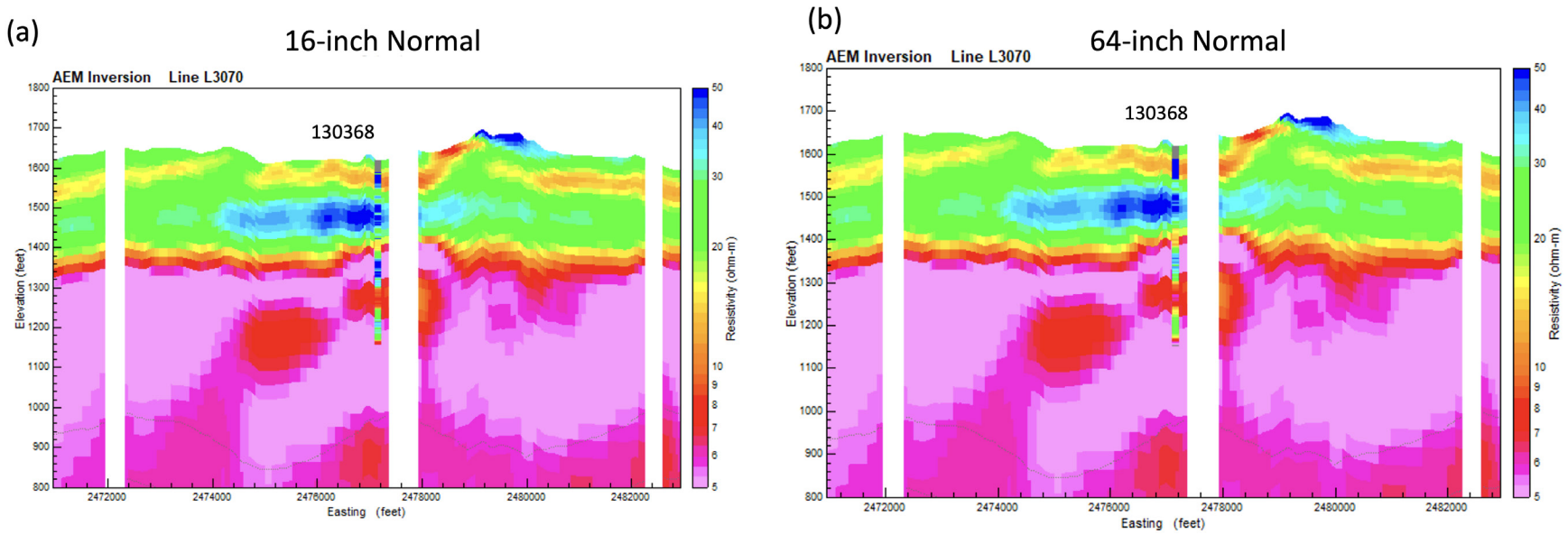

Figure 7-21. A comparison of the SCI inversions of line L3070 flown over test hole *130368* for both the (a) 16-inch Short Normal and (b) 64-inch Long Normal within the Griggs Block AEM survey area.

7.7.2 Towner Block AEM Survey Area

The structure of the subsurface Quaternary deposits of the Towner Block AEM survey area is dominated by the presence of several systems of paleochannels. The resistive Quaternary sands and gravels in the paleochannels of the Towner Block contrast with the clay and shale of the bedrock and the Quaternary deposits. Several selected AEM profiles will be examined with the borehole lithology as a comparison to verify the results of the AEM calibration and inversion. This also serves as a guideline that can be used in the interpretation of the AEM results.

Figure 7-22 is a profile view of east-west Line L1470 located in the area north of Devils Lake south of Highway 2. Line L1470 has several discreet channelized deposits. There are several boreholes within a ¼ mile of the flight line, and they show good matches to the conductive bedrock (shale) indicated by the AEM. They also show good correlation with the sediments along the line. Additionally, there is a resistive paleochannel that is imaged within the section at approximately Easting 2334000 (feet) that also has well number 9687. Several other channels that do not have wells in them are along the profile.

Figure 7-23 is a profile view of east-west Line L1250, located in the central portion of the Towner Block AEM survey area just south of Cando, North Dakota. There are many boreholes within a ¼ mile of the flight line that show good matches to the AEM bedrock as well as the lithology. One well, *27303*, penetrates a deeper paleochannel at approximately Easting 2255750. There is also an indication of another paleochannel at approximately Easting 2272500.

Figure 7-24 is a profile view of the northwest-southeast tie-line L2005, located along the length of the Towner Block AEM survey area. There are many boreholes within a ¼ mile of the flight line that show good matches to the AEM bedrock as well as the lithology. There are four wells that do not match the bedrock very well including *9917*/*9918* (at the same location), *9909*, and *10901*. These wells show that the bedrock is higher as compared with the AEM. These wells may need to be inspected for position error or errors in logging as many other wells match in the area.

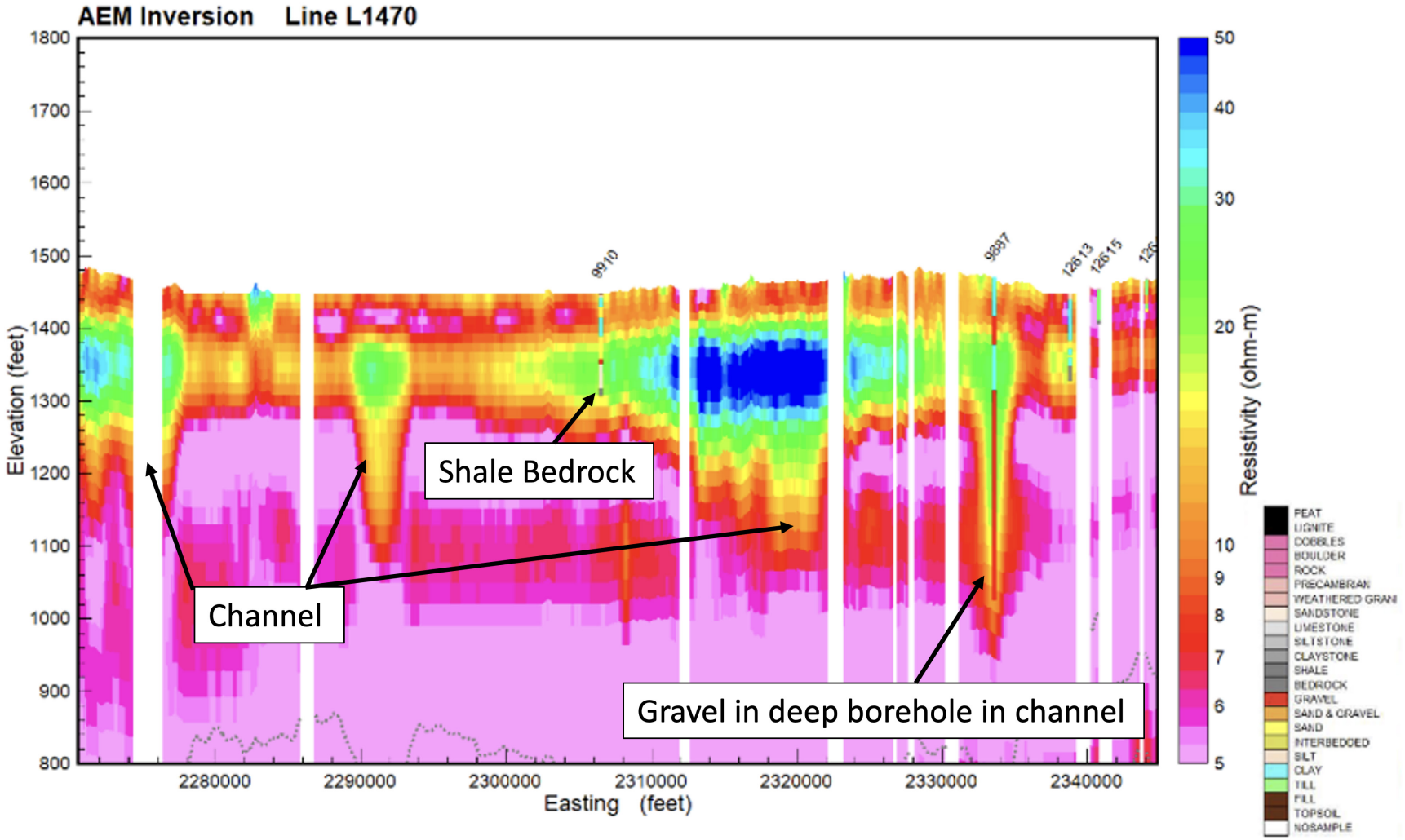

Figure 7-22. East-west flight line L1470 within the southern portion of the Towner Block AEM survey area.

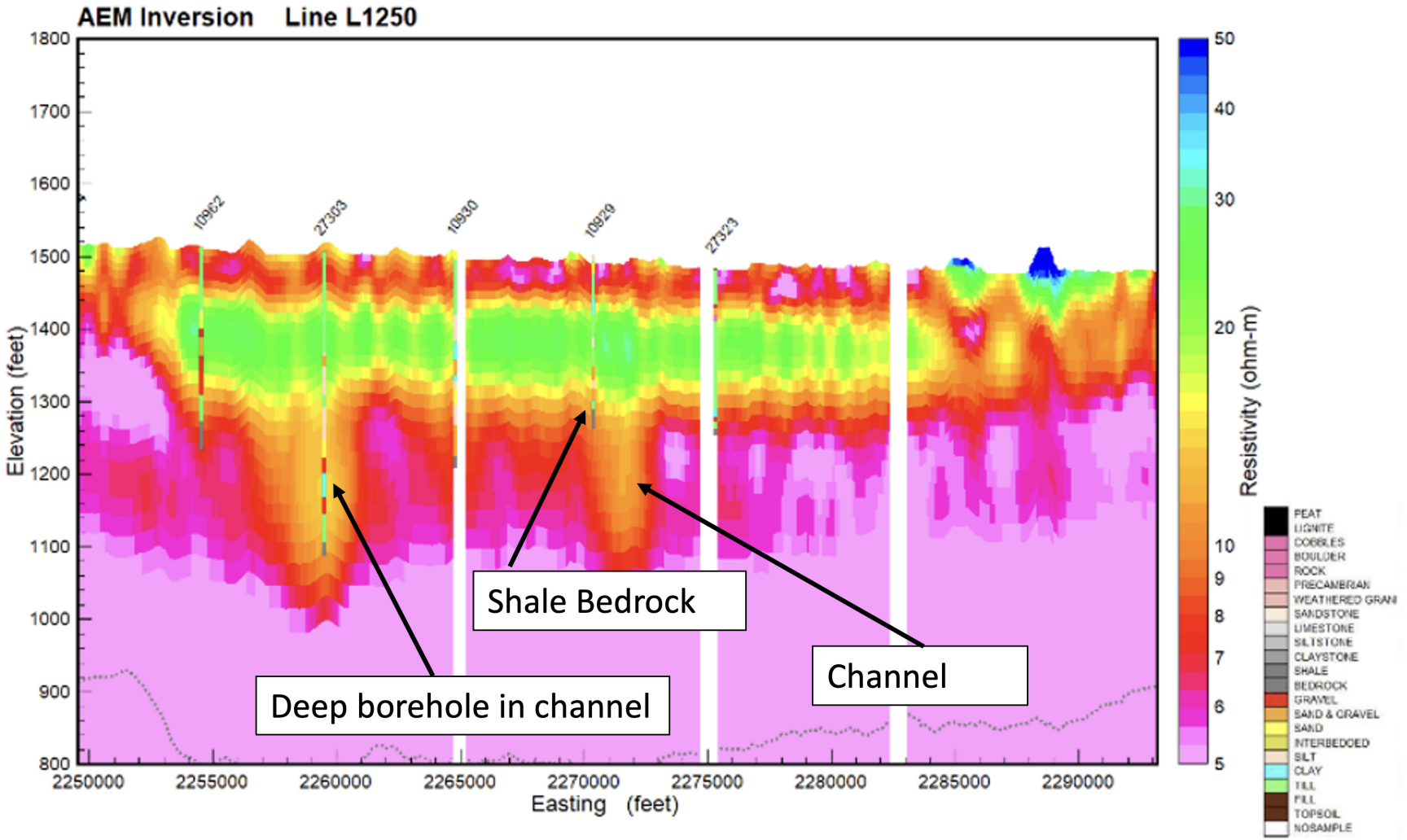

Figure 7-23. East-west flight line L1250 within the middle portion of the Towner Block AEM survey area.

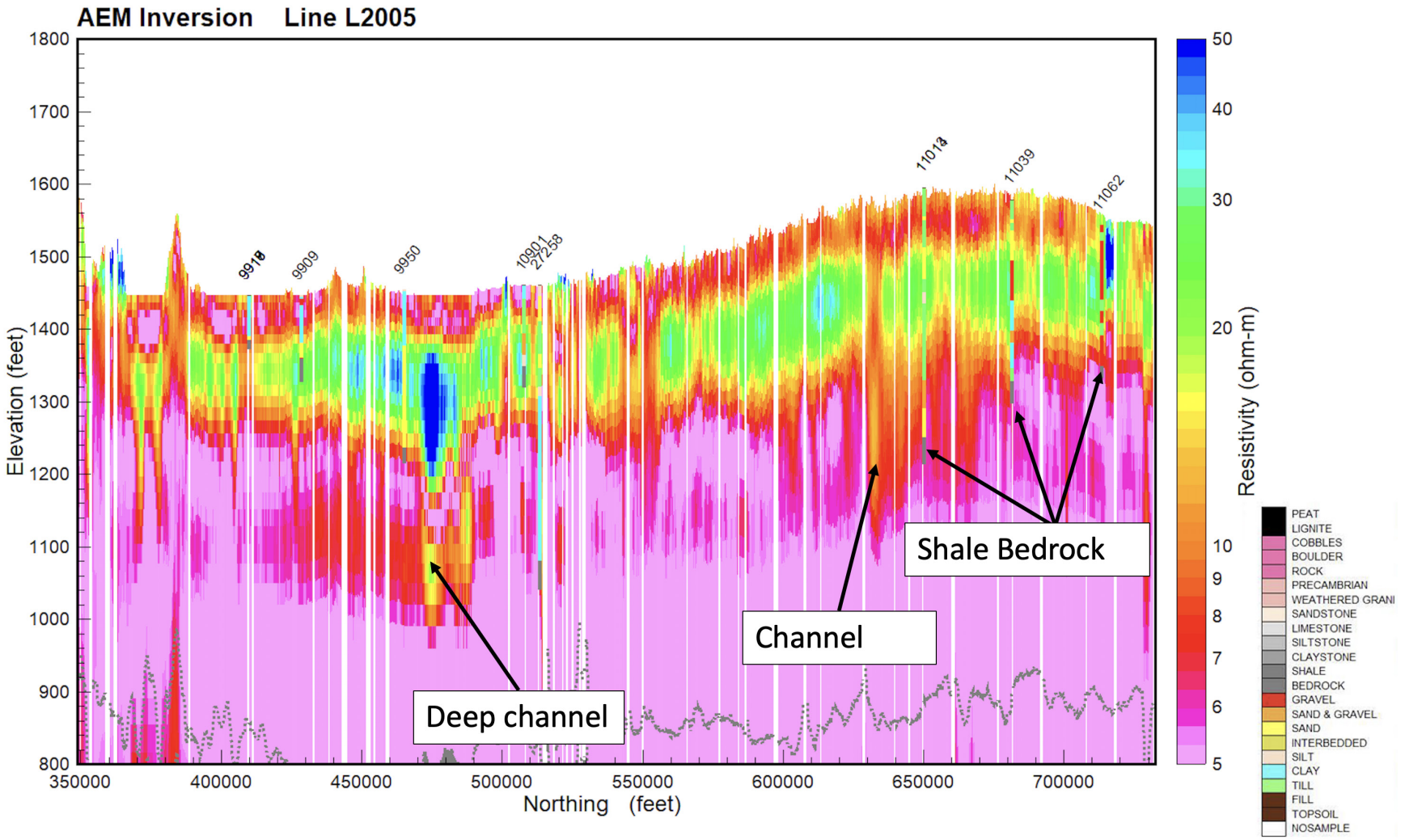

Figure 7-24. Northwest-southeast flight line L2005 along the length of the Towner Block AEM survey area.

7.7.3 Griggs Block AEM Survey Area

The dominant features in the Griggs Block AEM survey area are the large resistive paleochannel deposits. There are several cross-cutting resistors within the survey area at different elevations.

Figure 7-25 is a profile view of the AEM resistivity inversion along Line L3110 in the northern part of the Griggs Block AEM survey area. There are several boreholes that penetrate into the sand and gravels of the paleochannel and also indicate the bedrock. Well *6401* penetrates a paleochannel system. The log indicates sands that correlate well with the high resistivity zone. In the region of the resistive channels there is also a possible deeper channel at approximate Easting 2485000. This feature is right along an EM-coupling feature that was removed from the data.

Figure 7-26 is a profile view of the AEM resistivity inversion along Line L5250 in the central area of the Griggs Block AEM survey area. There are several boreholes that penetrate into the sand and gravels of the paleochannels and also indicate the bedrock. Well *6362* penetrates a deeper paleochannel system. The lithology logs indicate good correlate with the AEM resistivities.

Figure 7-27 is a profile view of northwest-southeast Line L4000, located along the northern portion of the length of the Griggs Block AEM survey area. There are many boreholes within a ¼ mile of the flight line and the show good matches to the AEM bedrock as well as the lithology. In the area of approximate Northing 240000 the AEM and the lithology logs indicate a deeper paleochannel below the larger channel system. This is the same area discussed above associated with the E-logs. There is also an odd well, *19081*, that is indicating a shale where the AEM indicates resistive materials. Overall, the correlations are very good along the flight line.

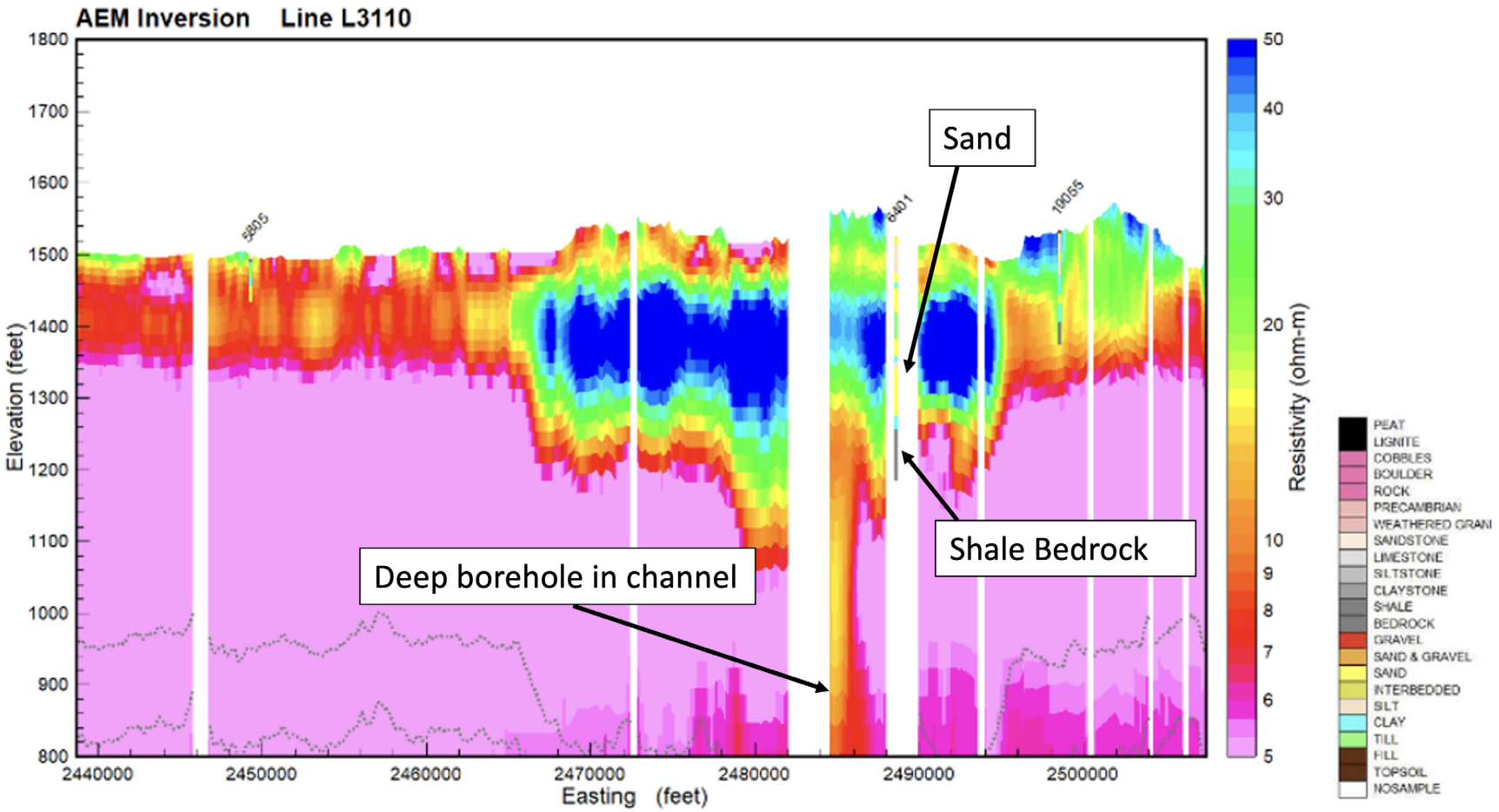

Figure 7-25. East-west flight line L3110 within the northern portion of the Griggs Block AEM survey area.

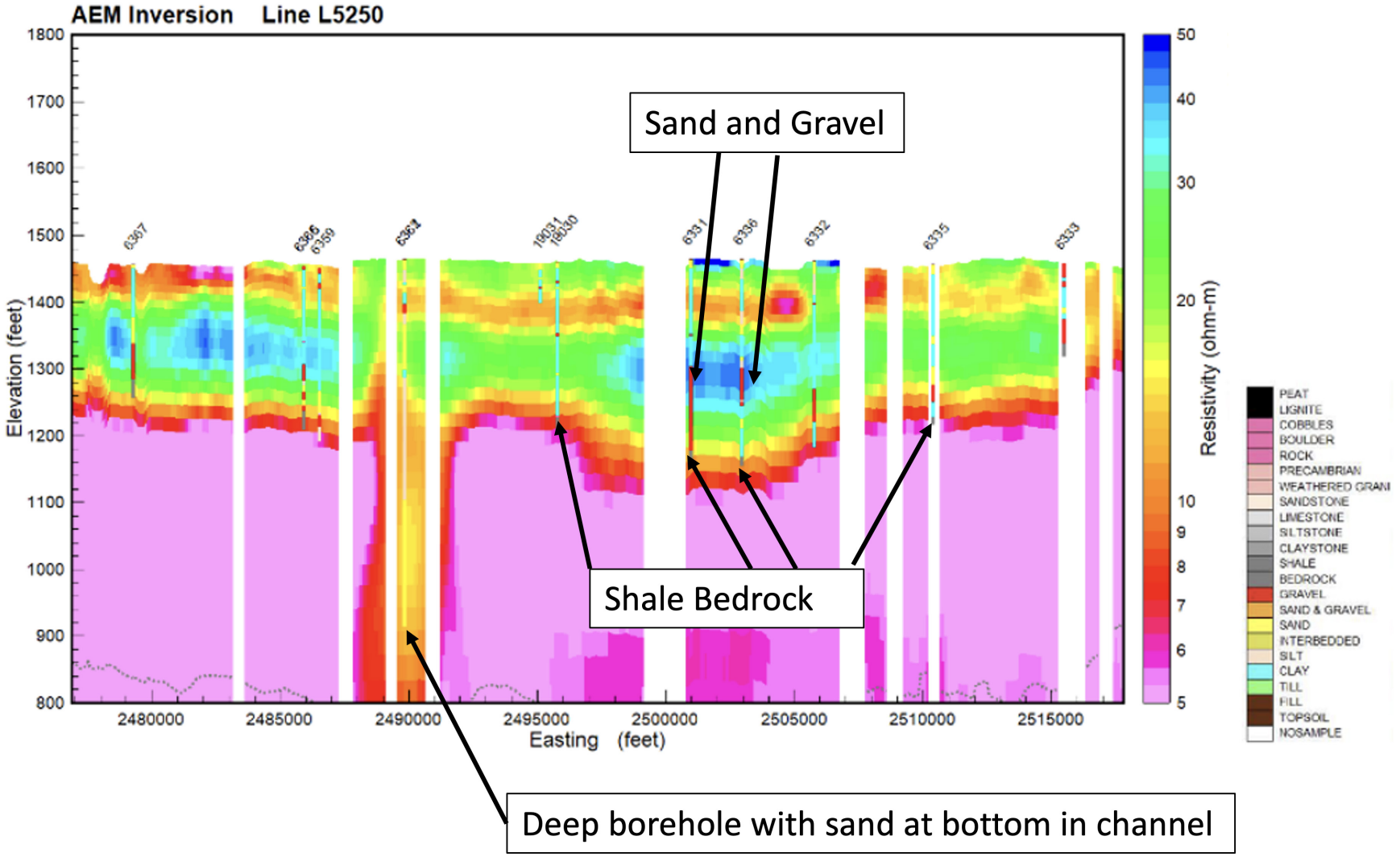

Figure 7-26. East-west flight line L5250 within the middle portion of the Griggs Block AEM survey area.

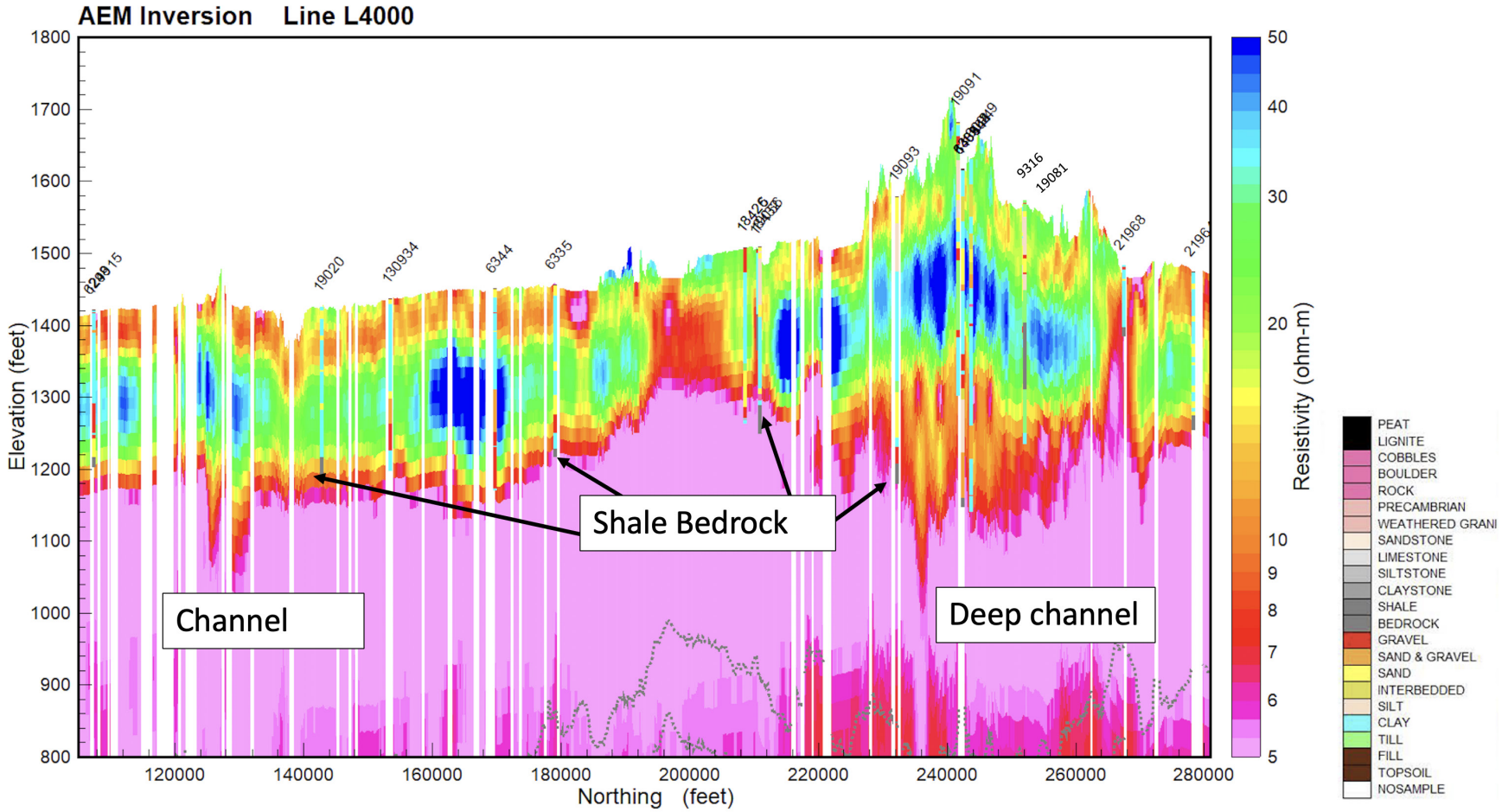

Figure 7-27. Northwest-southeast flight tie-line L4000 along the length of the Griggs Block AEM survey area.

7.8 Suggestions on Interpretation

The 2019 NDSWC Towner and Griggs Blocks AEM survey areas provide rich details on the geology from the surface down to the Cretaceous basement. Even so, care needs to be exercised in the interpretation of the resistivity, keeping in mind the limitations of the AEM resolution and quality of the borehole lithologies. Care also needs to be used around the areas of EM-coupling as some of the areas may show impacts of pull ups in the conductive basement. This is a consequence of attempting to leave as much acquired data as possible in the inversion. The EM coupling has an impact at the later times of adding to the conductive units. There will be no impact in the shallower depths. It is a tradeoff that needs to be understood in areas that may have pull-ups around EM-coupling cut outs.

The first suggestion in interpreting this dataset is to delineate the Cretaceous bedrock units. The next step would be to utilize resistivity thresholds on the Quaternary to identify the sand and gravel aquifers within the area. Another powerful technique is to adjust the resistivity color ramp to bring the details of the resistivity changes out of the Quaternary units without the need to display the Cretaceous low resistivity units.

Another suggestion related to interpretation of the multiple paleochannel deposits is to utilize the profiles and elevation layers to begin to pull out individual channel systems by digitizing their locations in X, Y, and Z and classifying the features as a specific system. Then begin to layer the systems from bottom to top by adjusting the classification of the channel system as needed.

8. Summary

This final report presents the Quality Assurance and Quality Control procedures, and the results of that analysis, that were applied to the setup and data acquisition of the airborne electromagnetic survey of NDSWC Towner and Griggs Blocks AEM survey areas. It also includes the preliminary LCI analysis, final SCI inversion results, and the SCI comparisons to E-logs and to lithology logs.

The QA/QC analysis included airborne testing of the system, the as-flown flight lines, and the flight altitude as the data was acquired. In addition, the power line noise monitor and magnetic field data were also examined and found to present no indications of any system or data acquisition issues. This first step included the generation of LCI inversions.

The final SCI results are presented as 2D resistivity profiles, 3D fence diagrams, 3D voxels, depth layers, and elevation layers. Google Earth KMZ files including the as flown-retained flight lines, the residual errors in the inversion, and the resistivity depth and elevation slices. A link to the DropBox location of these files is presented below.

We believe that given the challenge of the infrastructure in the Towner and Griggs Blocks AEM survey areas, these results provide a good, solid starting point for development of a hydrogeologic framework of the survey areas.

Dropbox Link:

https://www.dropbox.com/sh/1jswedygoy10wc9/AACMC2JWKfgUOKCfZYFgietAa?dl=0

9. Deliverables

In the Appendix 3 - Deliverables folder are five subfolders entitled Grids, KMZs, Processed Data, Raw Data, and Voxel.

Table 9-1 lists the channels in calibrated raw data files (Geosoft gdb's) provided by Geotech for both the Towner and Griggs AEM survey areas. Table 9-2 lists the channels in the final measured waveforms provided by Geotech as a combined Geosoft gdb. The combination of these two were input as raw data into the analysis software. These data are included in the *Raw Data* folder with the Final Waveforms in a separate sub-folder.

Table 9-3 presents the channels in the Towner and Griggs AEM survey SCI inversion results. These are provided as both Geosoft gdb and ASCII xyz data files. These data are included in the ***Processed Data*** folder.

Table 9-4 lists the delivered grids. in ArcView *.FLT format. These data are included in the ***Grids*** folder. In the *Grids* folder are six (6) subfolders: *DOI*, *DEM*, *Griggs_DepthLayers*, Griggs_ElevationLayers, Towner_DepthLayers, and Towner_ElevationLayers. The *DOI* folder contains grids of the upper and lower DOI's for both the Towner and Griggs AEM survey areas. The *DEM* folder contains the Digital Elevation Model grids for both the Towner and Griggs areas. The other four *Grids* sub-folders contain their own subfolders for both the Towner and Griggs areas that display the SCI inversion results in two ways: 1) Depth slice grids with each depth being a SCI model layer as per Table 5-1 and 2) Elevation slice grids with each depth being an elevation above sea level.

The Resistivity Depth Slice and Elevation Slice data are provided as grids as described and also as Google Earth ***KMZ***'s and as multi-layer ***PDF*** files. The KMZ and PDF data are provided with red to blue color scheme.

Table 9-5 list the channels in the delivered voxel data files for both the Towner and Griggs AEM survey areas. The files are provided as both ASCII xyz in the ***Voxel*** folder.

The *KMZ* folder contains the resistivity depth and elevation slices as described above and also the As-Flown-Retained data for both the Towner and Griggs AEM survey areas.

Table 9-1: Calibrated raw data: Channel name, description, and units for GL170349C_Towner_Final.gdb and GL170349C_Griggs_Final.gdb.

Parameter	Description	Unit
X	Easting WGS84/UTM 14 North	Meters (m)
Y	Northing WGS84/UTM 14 North	Meters (m)]
Z	Aircraft elevation (Above Geoid)	Meters (m)]
X_NAD83ft	Easting in NAD83, ND North zone, Intl ft	
Y_NAD83ft	Northing in NAD83, ND North zone, Intl ft	
Longitude	GPS Longitude	Degrees
Latitude	GPS Latitude	Degrees
DEM	Estimated elevation above Geoid	Meters [m]
RADAR	Helicopter terrain clearance	Meters [m]
RADARB	EM bird terrain clearance	Meters (m)
GTIME	Seconds of GPS time	Seconds (s)
BASEMAG	Magnetic field diurnal variation data	Nanoteslas (nT)
MAG1L, MAG1R, MAG2LZ, MAG2RZ	Raw Magnetic field data	Nanoteslas (nT)
TMI2, TMI3	Total Magnetic Field Intensity	Nanoteslas (nT)
TMI_RES	Total Magnetic Field Intensity Residual	Nanoteslas (nT)
CVG	Calculated Vertical Gradient of the Magnetic Field	nT/m
SFZ[4] – SFZ[46]	dB/dt data for gates 4 to 46	picoVolts/A*m^4
PLM	60 Hz Power Line Monitor	
TAUSF	Time constant	
TAUBF	Time constant	
NCHANSF	Number of Channels for SF	

Table 9-2. Raw Data: Transmitter waveforms by flight (1 to 26) in a Geosoft database gdb.

Parameter	Description	Unit
Time	Transmitter waveform time	milliseconds (ms)
Tx-Current	Measured Tx waveform voltage	Volts (v)]

Table 9-3. Channel name, description, and units for Towner_SCI.gdb, Griggs_SCI.gdb, and *.xyz files with AEM inversion results.

Parameter	Description	Unit
LINE	Line Number	Feet [ft]
X_FT	Easting NAD83, State Plane North Dakota, North	Int. Feet [ft]
Y_FT	Northing NAD83, State Plane North Dakota, North	Int. Feet [ft]
ELEVATION_M	Elevation of Inversion Surface	Meters [m]
DEM_FT	DEM from 100 ft grid NED NAVD88	Feet [ft]
DISTANCE_FT	Distance down line	Feet [ft]
X_M	Easting NAD83, UTM Zone 14	Meters [m]
Y_M	Northing NAD83, UTM Zone 14	Meters [m]
DEM_M	DEM from survey	Meters [m]
DISTANCE_M	Distance down line	Meters [m]
FID	Unique Fiducial Number	
TIME	Date Time Format	Decimal days
ALT_M	Altitude of system above ground	Meters [m]
INVALT	Inverted Altitude of system above ground	Meters [m]
INVALTSTD	Inverted Altitude Standard Deviation of system above ground	Meters [m]
RESDATA	Residual of individual sounding	
RESTOTAL	Total residual for inverted section	
DOI_UPPER_FT	More conservative estimate of DOI	Feet [ft]
DOI_LOWER_FT	Less conservative estimate of DOI	Feet [ft]
DOI_UPPER_M	More conservative estimate of DOI	Meters [m]
DOI_LOWER_M	Less conservative estimate of DOI	Meters [m]
RHO_I_0 THROUGH RHO_I_38	Inverted resistivity of each later	Ohm-m
RHO_STD_0 THROUGH RHO_STD_38	Inverted resistivity standard deviation	
SIGMA_I_0 THROUGH SIGMA_I_38	Conductivity	S/m
DEP_TOP_FT_0 THROUGH DEP_TOP_FT_38	Depth to the top of individual layers	Feet [ft]
DEP_BOT_FT_0 THROUGH DEP_BOT_FT_38	Depth to the bottom of individual layers	Feet [ft]
THK_FT_0 THROUGH THK_FT_38	Thickness of individual layers	Feet [ft]
DEP_TOP_M_0 THROUGH DEP_TOP_M_38	Depth to the top of individual layers	Meters [m]
DEP_BOT_M_0 THROUGH DEP_BOT_M_38	Depth to the bottom of individual layers	Meters [m]
THK_M_0 THROUGH THK__M_38	Thickness of individual layers	Meters [m]

Table 9-4. Files containing ESRI ArcView Binary Grids *.flt.

Grid File Name	Description	Grid Cell Size (feet)
Towner_DOI_Lower_ft	**Towner Block grid of the lower depth of investigation (DOI) (feet) NAD83, State Plane North Dakota, North (Int. ft)**	**500**
Towner_DOI_Upper_ft	**Towner Block grid of the upper depth of investigation (DOI) (feet) NAD83, State Plane North Dakota, North (Int. ft)**	**500**
Griggs_DOI_Lower_ft	**Griggs Block grid of the lower depth of investigation (DOI) (feet) NAD83, State Plane North Dakota, North (Int. ft)**	**500**
Griggs_DOI_Upper_ft	**Griggs Block grid of the upper depth of investigation (DOI) (feet) NAD83, State Plane North Dakota, North (Int. ft)**	**500**
ND19_Towner_RHO_LayerXX	**Towner Block Resistivity grids of the 39 inverted model depth layers (ohm-m), NAD83, State Plane North Dakota, North (Int. ft)**	**500**
ND19_Griggs_RHO_LayerXX	**Griggs Block Resistivity grids of the 39 inverted model depth layers (ohm-m), NAD83, State Plane North Dakota, North (Int. ft)**	**500**
Towner_XXXft_XXX	**Towner Block Elevation Resistivity (ohm-m) grids, from 300 to 1,700 feet NAVD88, NAD83, State Plane North Dakota, North (Int. ft)**	**500**
Griggs_ XXXft_XXX	**Griggs Block Elevation Resistivity (ohm-m) grids, from 300 to 1,700 feet NAVD88, NAD83, State Plane North Dakota, North (Int. ft)**	**500**
NDSWC_DEM_Extended_100ftres	**Grid of the USGS National Elevation Dataset (NED) digital elevation model (DEM) NAVD88 (feet), NAD83, State Plane North Dakota, North (Int. ft)**	**100**

Table 9-5. Channel name, description, and units for Towner_Res_voxel.csv and Griggs_Res_voxel.csv.

Parameter	Description	Unit
X	Easting NAD83, State Plane North Dakota North	Int. Foot [ft]
Y	Northing NAD83, State Plane North Dakota North	Int. Foot [ft]
Z	Elevation of Voxel Node	NAVD88 [ft]
Rho_I	Voxel cell resistivity value of the Inverted AEM Model	Ohm-m

10. References

Aarhus Geosoftware, 2020 Aarhus Workbench, available on the world-wide web at: https://www.aarhusgeosoftware.dk/aarhus-workbench (accessed February 27, 2020)

Asch, T.H., Abraham, J.D., and Irons, T., 2015, "A discussion on depth of investigation in geophysics and AEM inversion results", Presented at the Society of Exploration Geophysicists Annual Meeting, New Orleans.

Auken, E., Christiansen, A.V., Kirkegaard, C., Fiandaca, G., Schamper, C., Behroozmand, A.A., Binley, A., Nielsen, E., Effersø, F., Christensen, N.B., Sørensen, K., Foged, N., and Vignoli, G., 2015, An overview of a highly versatile forward and stable inverse algorithm for airborne, ground-based and borehole electromagnetic and electric data: Exploration Geophysics, Vol. 46, No. 3, 2015, p. 223-235, http://dx.doi.org/10.1071/EG13097

Christensen, N. B., Reid, J. E., and Halkjaer, M., 2009, "Fast, laterally smooth inversion of airborne time-domain elecromagnetic data." *Near Surface Geophysics* 599-612.

Christiansen, A. V., and E. Auken, 2012, "A global measure for depth of investigation." *Geophysics,Vol. 77, No. 4* WB171-177.

Christiansen, A.V., Auken, E., Kirkegaard, C., Schamper, C., Noel, C., Vignoli, G., 2016, An efficient hybrid scheme for fast and accurate inversion of airborne transient electromagnetic data: Exploration Geophysics, Vol. 47, No. 4, 2016, p. 331-340, http://dx.doi.org/10.1071/EG14121

DatamineDiscover, 2020, Datamine Discover Profile Analyst, available on the world-wide web at: https://www.dataminesoftware.com/solutions/discover-exploration-gis/ (accessed on February 27, 2020).

Geosoft, 2020, Oasis montaj software, https://www.geosoft.com/products/oasis-montaj

Geotech LTD., 2019,VTEM (Versatile Time Domain Electromagnetic) System, available on the world-wide web at: http://geotech.ca/services/electromagnetic/vtem-versatile-time-domain-electromagnetic-system/ (accessed November 19, 2019).

Legault, J.M., Eadie, T., Plastow, G., Prikhodko, A., Hisz, D., and Patch, J., 2018, Characterizing the Spiritwood Valley Aquifer, North Dakota, using helicopter time-domain EM: ASEG Extended Abstracts, 2018:1, 1-5, https://doi.org/10.1071/ASEG2018abT4_1H

Legault, J.M., Asch, T.H., Hisz, D., Khaled, K., Abraham, J.D., Parkin, H.S., and Honeyman, R.P., 2019, Further characterization of the Spiritwood Valley Aquifer in North Dakota using helicopter time domain electromagnetics: in Abstracts from the 32nd Symposium on the Application of Geophysics to Engineering and Environmental Problems, Portland, OR, March 18, 2019. http://earthdoc.eage.org/publication/search?pubsearchkey=Electromagnetics&sortby=publicationtype&sortlang=1

North Dakota State Water Commission, 2019, Map Services, available on the world-wide web at: http://mapservice.swc.nd.gov (accessed November 16, 2019).

Sapia, V, Oldenborger, G.A., Jorgenson, F., Pugin, A.J-M., Marchetti, M, and Viezzoli, A., 2015, 3D modeling of buried valley geology using airborne electromagnetic data: Interpretation, Vol 3, No.4, p. SAC9-SAC22. http://dx.doi.org/10.1190/INT-2015-0083.1

U.S. Geological Survey (USGS), 2019, The National Map, 2019, 3DEP products and services: The National Map, 3D Elevation Program Web page, https://www.usgs.gov/core-science-systems/ngp/3dep/about-3dep-products-services (accessed February 28, 2020).

Viezzoli, A., Christiansen, A. V. , Auken, E., and Sorensen, K., 2008, "Quasi-3D modeling of airborne TEM data by spatially constrainted inversion." *Geophysics Vol. 73 No. 3* F105-F11